

**NASA CONTRACTOR  
REPORT**



**NASA CR-2405**

**NASA CR-2405**

**DIFFRACTION BY A PERFECTLY CONDUCTING  
RECTANGULAR CYLINDER WHICH IS ILLUMINATED  
BY AN ARRAY OF LINE SOURCES**

*by R. G. Kouyoumjian and N. Wang*

*Prepared by*

**THE OHIO STATE UNIVERSITY  
ELECTROSCIENCE LABORATORY**

**Columbus, Ohio 43212**

*for Langley Research Center*



**NATIONAL AERONAUTICS AND SPACE ADMINISTRATION • WASHINGTON, D. C. • JUNE 1974**

1. Report No. NASA CR- 2405		2. Government Accession No.		3. Recipient's Catalog No.	
4. Title and Subtitle  DIFFRACTION BY A PERFECTLY CONDUCTING RECTANGULAR CYLINDER WHICH IS ILLUMINATED BY AN ARRAY OF LINE SOURCES				5. Report Date June 1974	
				6. Performing Organization Code	
7. Author(s)  R. G. Kouyoumjian and N. Wang				8. Performing Organization Report No.  TR 3001-7	
9. Performing Organization Name and Address  The Ohio State University ElectroScience Laboratory Columbus, Ohio 43212				10. Work Unit No.  502-33-13-02	
				11. Contract or Grant No.  NGR 36-008-144	
12. Sponsoring Agency Name and Address  National Aeronautics and Space Administration Washington, D.C. 20546				13. Type of Report and Period Covered  Contractor Report	
				14. Sponsoring Agency Code	
15. Supplementary Notes  Topical report.					
16. Abstract  The geometrical theory of diffraction (GTD) is employed to analyze the radiation from a perfectly-conducting rectangular cylinder illuminated by an array of line sources. The excitation of the cylinder by a single electric or magnetic current line source is considered first, and a solution which includes contributions from the geometrical optics rays and all singly- and doubly-diffracted rays is obtained. A new diffraction coefficient valid in the transition regions of the shadow and reflection boundaries is employed to obtain a continuous total field, except for negligible discontinuities in the doubly-diffracted field at its shadow boundaries. Patterns calculated by the GTD method are found to be in excellent agreement with those calculated from an integral equation formulation. Using superposition the solution for array or aperture excitation of the rectangular cylinder is obtained. A computer program for this solution is included.					
17. Key Words (Suggested by Author(s))  Antenna, Spacecraft and Aircraft Antennas  Applied Electromagnetic Theory				18. Distribution Statement  Unclassified - Unlimited   STAR Category 09	
19. Security Classif. (of this report)  Unclassified	20. Security Classif. (of this page)  Unclassified	21. No. of Pages  71	22. Price*  \$3.75		

**Page Intentionally Left Blank**

# TABLE OF CONTENTS

	Page
	1
II. METHOD OF SOLUTION	3
A. Geometrical Optics Rays - Direct and Reflected	3
B. Singly-Diffracted Rays	5
C. Doubly-Diffracted Rays	7
III. NUMERICAL RESULTS	18
IV. CONCLUSIONS	26
APPENDIX I	
THE FIELD AT THE SHADOW BOUNDARY OF A THICK SCREEN FOR GRAZING INCIDENCE	27
APPENDIX II	
DESCRIPTION OF THE COMPUTER PROGRAM	31
A. Input Variables	31
B. Output Variables	31
C. Instructions for Representing the Aperture Field Distribution by a 2-D Line Source Array	32
D. Instructions for Using the "Obliquity Factor"	34
E. Instructions for Computing the Incident Field	34
F. Sample Programs	35
G. Listing of the Computer Programs	40
REFERENCES	69

## I. INTRODUCTION

In this report the geometrical theory of diffraction (GTD) [1] is used to treat the diffraction by a perfectly-conducting rectangular cylinder which is illuminated by an array of electric or magnetic current line sources. The illumination by a single line source of the array is considered first with the geometry of the problem shown in Fig. 1. The scattered and total fields are calculated at all points exterior to the rectangular cylinder, except for the shaded regions around the source and edges, which are excluded because of the nature of the high-frequency approximation. More will be said about this later. The solution is then generalized to calculate the field of linear arrays of such line sources radiating in the presence of the cylinder.

The scattering by a rectangular cylinder has been considered previously for the special case of plane wave incidence. Mei and VanBladel [2,3] formulated the problem in terms of an integral equation which they solved numerically to find the surface currents on the rectangular cylinder. They give radiation patterns, scattering cross sections, and surface currents for both E- and H-polarized incident waves. There are two disadvantages associated with this method: 1) as the frequency increases, difficulties are encountered with the convergence of the solution (this is particularly true when the technique is employed to solve a three-dimensional scattering problem), 2) the solution provides no physical insight into the scattering mechanism. Morse [4] also studied this problem using the ordinary GTD to obtain expressions for the diffracted field away from shadow and reflection boundaries. Since the ordinary theory fails at shadow and reflection boundaries, he introduced supplementary solutions there. He employed Oberhettinger's uniform asymptotic solution [5] near the boundaries of the incident and reflected fields, and he employed an integral representation of the field near the shadow boundaries of the fields of the diffracted rays. Thus, he did not obtain a compact high-frequency solution to this problem. The difficulties encountered by Morse at these boundaries may be overcome with a new edge diffraction coefficient derived by Kouyoumjian and Pathak [6,7]. This diffraction coefficient can be applied in the transition regions adjacent to the shadow and reflection boundaries so that one obtains a total field which is valid and continuous everywhere away from edges and caustics. Their diffraction coefficient is employed in this analysis.

Using Keller's Generalized Fermat's Principle, we include contributions to the total field from the geometrical optics fields (incident and reflected), as well as singly-diffracted fields which appear to emanate from the edges. Doubly-diffracted fields have also been included to describe the interactions between the edges; however, multiply-diffracted rays of higher order have been neglected because, in general, their fields contribute insignificantly, for the problem defined here. The incident, reflected and diffracted rays may be shadowed in the geometrical optics sense, and hence they contribute to the total field only in their respective regions of illumination. Discontinuities in the

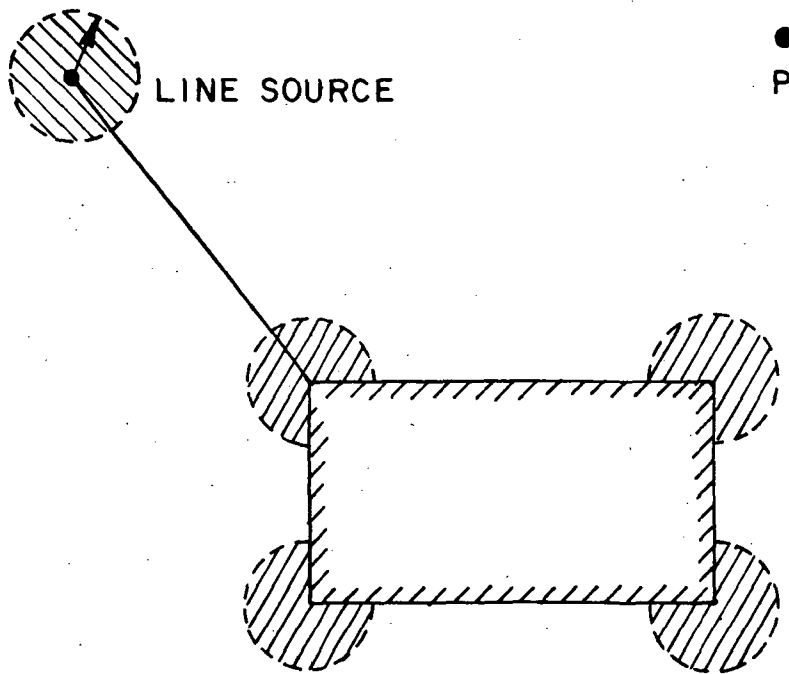


Fig. 1. Line source in the presence of the rectangular cylinder.

field are introduced at shadow boundaries and at the reflection boundaries, but they are systematically removed by employing the new diffraction coefficient for the edge diffracted field mentioned previously. It should be pointed out that there are some residual discontinuities due to uncompensated discontinuities in the field of the doubly-diffracted rays at their shadow boundaries. However, these discontinuities are so small that they are not apparent in the plotted patterns. The patterns calculated from our GTD solution are found to be in excellent agreement with those calculated from numerical solutions.

Due to the high-frequency approximations of the incident and diffracted fields, our solution is restricted so that the following distances are greater than 0.7 wavelength.

- 1) The distance between the line source and the closest edge of the rectangular cylinder,
- 2) the distance between the observation point P and the closest edge of the rectangular cylinder,
- 3) the distances between the edges of the rectangular cylinder,
- 4) the distance between the observation point P and the closest line source, when calculating the incident or total fields.

A computer program based on the GTD solution for the rectangular cylinder in the presence of an array source has been written and is included in the report. With this program, it is possible to obtain numerical results for both the near- and far-fields of the cylinder under quite general conditions of illumination. Thus, the program is directly relevant to both antenna and scattering problems. As an example of its versatility, one notes that the program may be used to compute the pattern of an array of magnetic line sources mounted directly on the rectangular cylinder, provided the sources are not too close to an edge.

## II. METHOD OF SOLUTION

Keller's geometrical theory of diffraction [1] is an extension of geometrical optics in which diffracted rays are introduced by a generalization of Fermat's principle, the excitation of the diffracted field is treated as a local phenomenon, and away from the diffracting surface the behavior of the diffracted field along its ray is the same as that of the geometrical optics field. The basic idea of GTD is that the field of the line source illuminates the rectangular cylinder giving rise to a reflected field and an edge diffracted field, which consists of the fields of singly and multiply-diffracted rays. The total field  $U(P)$  at a point  $P$  is equal to the sum of the fields on all rays through  $P$ .

$$(1) \quad U(P) = \sum_{\text{rays}} U_i(P)$$

which includes the incident field if  $P$  is not in the shadow region. The wave function  $U(P)$  represents a magnetic field parallel to the edge in case of a magnetic line source, and an electric field parallel to the edge in the case of an electric current line source. The pertinent rays and their associated fields will be discussed briefly in the following paragraphs.

### A. Geometrical Optics Rays - Direct and Reflected

Let us consider the field radiated from a line source at  $O$  and observed at  $P$  as shown in Fig. 2. Fermat's principle predicts only the direct ray  $OP$ . If a line source is being considered, the field along  $OP$  is given by

$$(2) \quad U^i(P) = C \frac{e^{-jk s_0}}{\sqrt{s_0}},$$

where  $s_0$  is the distance between  $O$  and  $P$ , and  $C$  is a conveniently chosen normalization constant. For the configuration shown in Fig. 2, the space surrounding the right-angle wedge may be divided into three regions:

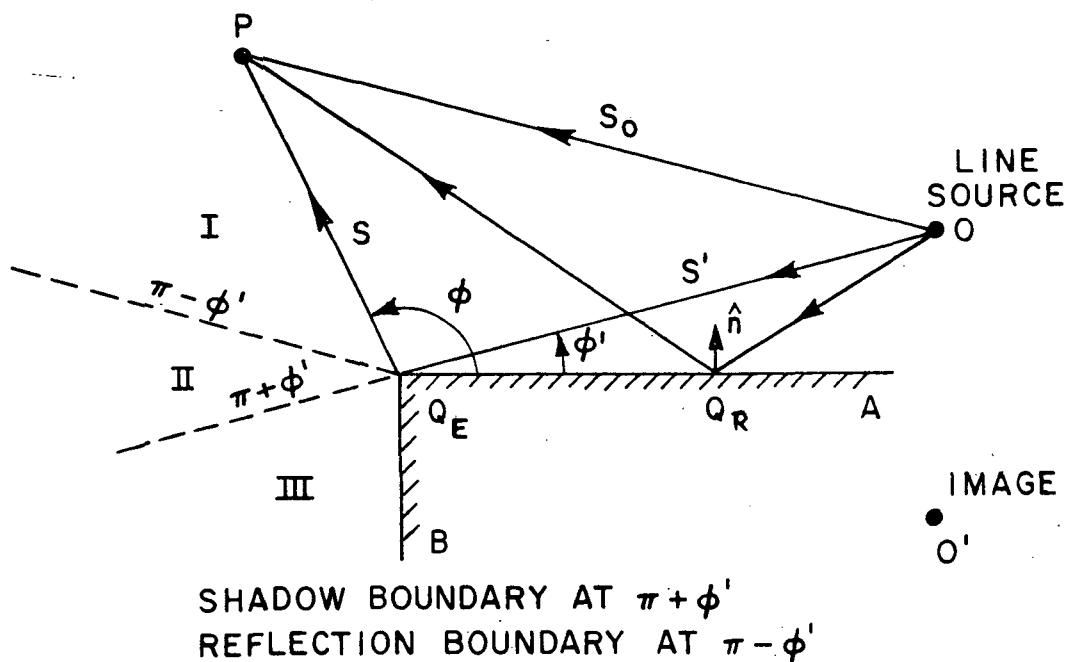


Fig. 2. Line source in the presence of a wedge.

Region I	$0 \leq \phi < \pi - \phi'$ ,
Region II	$\pi - \phi' < \phi < \pi + \phi'$ ,
Region III	$\pi + \phi' < \phi < 3\pi/2$ .

Region III is the shadow region, which is not penetrated by the incident ray; the incident field vanishes here.

We know that there is a field reflected from the surface  $AQ_E$ . To describe this we introduce an additional class of rays which include on their trajectory a point  $Q_R$  of the surface  $AQ_E$ . Applying Fermat's principle, the distance  $OQ_RP$  along the ray path is a minimum and the law of reflection results. This simple extension of Fermat's principle which accounts for the reflected ray is so natural that we accept it without question. The field of the reflected ray is readily deduced from image theory as

$$(3) \quad U^r(P) \equiv U^r(A-Q_E) = \pm C \frac{e^{-jks''}}{\sqrt{s''}},$$

where the positive sign is for Neumann (hard) boundary condition associated with the magnetic current line source, the negative sign is for the Dirichlet (soft) boundary condition associated with the electric current source line, and  $s''$  is the distance between the image  $O'$  and the observation point  $P$ . The reflected field vanishes in regions II and III, which the reflected ray does not penetrate. Let us consider now a further extension of Fermat's principle.



## B. Singly-Diffracted Rays

It is well known that the ray incident on the edge  $Q_E$  in Fig. 2 gives rise to diffraction. To account for this, Keller introduced a class of rays which includes the point  $Q_E$  in its trajectory. This completely determines the diffracted ray path in the isotropic, homogeneous medium of this two-dimensional problem, so the law of edge diffraction becomes trivial under these circumstances.

In terms of GTD, the diffracted field at  $P$  for the line source at  $O$  is

$$(4) \quad U^d(Q_E) = U^i(Q_E) D_h(\phi, \phi') \frac{e^{-jks}}{\sqrt{s}},$$

where  $D_s$  is the scalar diffraction coefficient for the acoustically soft (Dirichlet) boundary condition and  $D_h$  is the scalar diffraction coefficient for the acoustically hard (Neumann) boundary condition. They are deduced from the general dyadic diffraction coefficient  $\bar{D}(\phi, \phi', \beta_0)$  obtained by Kouyoumjian and Pathak [6,7]. For the special case where the incident ray is perpendicular to a straight edge, the scalar diffraction coefficients are given by

$$(5) \quad D_h(\phi, \phi') = \frac{-e^{-j\pi/4}}{2n\sqrt{2\pi k}} \left\{ \left[ \cot\left(\frac{\pi+(\phi-\phi')}{2n}\right) F[kLa^+(\phi-\phi')] + \cot\left(\frac{\pi-(\phi-\phi')}{2n}\right) F[kLa^-(\phi-\phi')] \right] \right. \\ \left. \pm \left[ \cot\left(\frac{\pi+(\phi+\phi')}{2n}\right) F[kLa^+(\phi+\phi')] + \cot\left(\frac{\pi-(\phi+\phi')}{2n}\right) F[kLa^-(\phi+\phi')] \right] \right\}$$

where  $n\pi$  is the exterior wedge angle, which equals  $3\pi/2$  in this case, and

$$(6) \quad F(x) = 2j|\sqrt{x}| e^{jx} \int_{|\sqrt{x}|}^{\infty} e^{-j\tau^2} d\tau$$

in which

$$(7) \quad a^{\pm}(\phi \pm \phi') = 2 \cos^2\left(\frac{2n\pi N^{\pm} - (\phi \pm \phi')}{2}\right).$$

$N^\pm$  are the integers which most nearly satisfy the following equations

$$(8) \quad 2\pi n N^+ = \pi + (\phi \pm \phi')$$

$$(9) \quad 2\pi n N^- = -\pi + (\phi \pm \phi')$$

and  $kL$  is the large parameter in the asymptotic evaluation of the pertinent integrals involved in the derivation of the dyadic diffraction coefficient. The quantity  $L$  may be viewed as a distance parameter which depends upon the type of edge illumination; for line source illumination,  $L$  is given by

$$(10) \quad L = \frac{s s'}{s + s'}$$

For grazing incidence  $\phi' = 0$ ,  $n\pi$ ,  $D_h$  is multiplied by a factor of  $\frac{1}{2}$ ; furthermore, if the diffracted ray grazes the surface in the case of a soft boundary,  $D_s = 0$  and the diffracted field vanishes, as it should.

The field of the singly-diffracted ray is discontinuous at the shadow and reflection boundaries in a way which compensates the discontinuities in the geometrical optics fields there. This is readily demonstrated; consider for example the incident and diffracted fields at the shadow boundary, where to simplify the discussion, it is assumed there is no nearby reflection boundary. Let  $\pi + \phi' - \epsilon$  be a point close to the shadow boundary, see Fig. 2. In the illuminated region  $\epsilon > 0$  and in the shadow region  $\epsilon < 0$ .

$$(11) \quad U(\phi) = \begin{cases} C \frac{e^{-jks_0}}{\sqrt{s_0}} + C \frac{e^{-jks'}}{\sqrt{s'}} D_h(\phi' + \pi - \epsilon, \phi') \frac{e^{-jks}}{\sqrt{s}}, & \epsilon > 0 \\ C \frac{e^{-jks'}}{\sqrt{s'}} D_h(\phi' + \pi - \epsilon, \phi') \frac{e^{-jks}}{\sqrt{s}}, & \epsilon < 0 \end{cases}$$

For  $\epsilon$  small it follows from Eq. (5) that

$$(12) \quad D_h(\phi' + \pi - \epsilon, \phi') = \frac{-e^{-j\pi/4}}{2n\sqrt{2\pi k}} \left\{ \cot \frac{\epsilon}{2n} F[kLa^-(\pi - \epsilon)] \right. \\ \left. + \text{smaller terms which are continuous at the shadow boundary} \right\}.$$

From Eq. (9),

$$N^- = 0$$

Also, as  $\epsilon \rightarrow 0$ ,

$$(13) \quad \cot\left(\frac{\epsilon}{2n}\right) = \frac{2n}{\epsilon}$$

$$(14) \quad a^-(\pi-\epsilon) = \frac{\epsilon^2}{2}$$

$$(15) \quad F[kLa^-(\pi-\epsilon)] = \sqrt{\pi kL/2} e^{j\pi/4} |\epsilon|$$

Substituting Eqs. (13) and (15) into Eq. (12) as  $\epsilon \rightarrow 0$ ,

$$(16) \quad D_{\frac{S}{h}}(\phi' + \pi - \epsilon, \phi') = -\frac{1}{2} \sqrt{\frac{S' S}{S + S'}} \quad \text{sgn } \epsilon + \text{smaller, continuous terms,}$$

$$(17) \quad s_0 = s' + s$$

Upon substituting Eqs. (16) and (17) into Eq. (11), it is seen that the total field is continuous at the shadow boundary. In an analogous manner it can be shown that the total field is continuous at the reflection boundary.

### C. Doubly-Diffracted Rays

When one face of the conducting wedge is terminated at  $Q_F$  as shown in Fig. 3, a second order diffracted-ray will emanate from the edge  $Q_F$ . In terms of the GTD, the doubly-diffracted field at  $P$  due to the line source at  $O$  can be written as

$$(18) \quad U^d(Q_E, Q_F) = U^i(Q_F) \frac{1}{2} D_{\frac{S}{h}}(\phi_2, 0) \frac{e^{-jks}}{\sqrt{S}}$$

$$= \left\{ U^i(Q_E) D_{\frac{S}{h}}\left(\frac{3\pi}{2}, \phi'\right) \frac{e^{-jkh}}{\sqrt{h}} \right\} \frac{D_{\frac{S}{h}}(\phi_2, 0)}{2} \frac{e^{-jks}}{\sqrt{S}}$$

Since  $D_s(3\pi/2, \phi') = 0$ , the contribution from the doubly-diffracted rays vanishes for the soft boundary according to the above expression. If a higher order approximation for the doubly-diffracted field is employed, then this contribution is non-vanishing, as will be explained later.

The field of the ray singly-diffracted at  $Q_E$  has a shadow boundary  $SB(Q_E)$  as shown in Fig. 3; the singly-diffracted ray does not penetrate

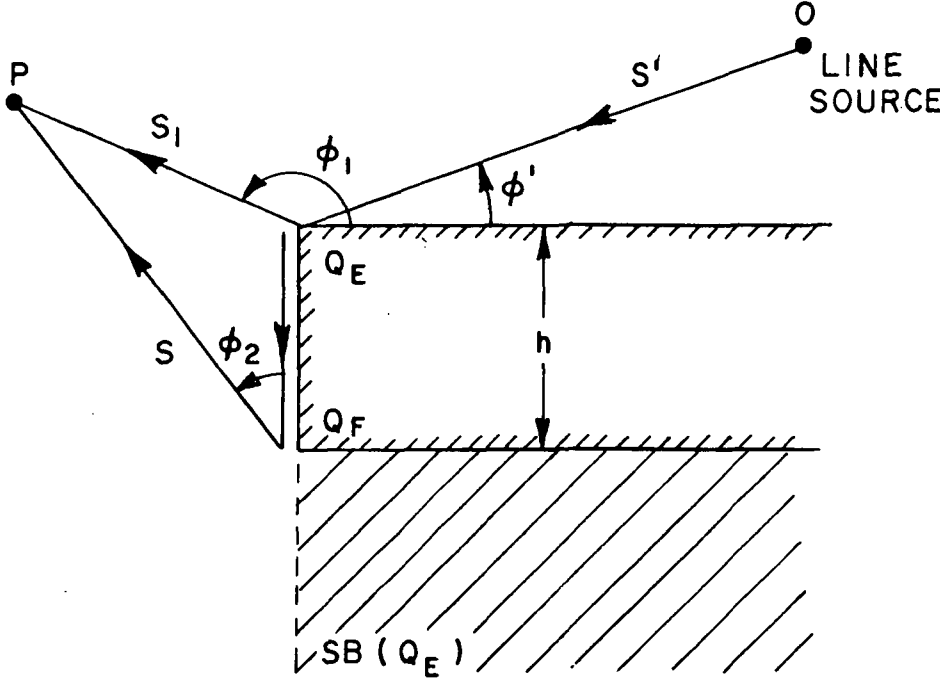


Fig. 3. Configuration for double-diffraction.

the shaded region. It will be shown next that the discontinuity in the field of the singly-diffracted ray at  $SB(Q_E)$  is compensated by the ray doubly-diffracted from  $Q_F$ , so that the total diffracted field is continuous at this boundary. Since the field doubly diffracted vanishes in the case of the soft boundary, we only need to treat the hard boundary here.

Consider a point close to  $SB(Q_E)$  so that  $\phi_2 = \pi - \epsilon$ , the total diffracted field at this boundary is

$$(19) \quad U^{TD} = \begin{cases} U^i(Q_E) D_h(\phi_1, \phi') \frac{e^{-jks_1}}{\sqrt{s_1}} + U^i(Q_F) \frac{D_h(\pi - \epsilon, 0)}{2} \frac{e^{-jks}}{\sqrt{s}}, & \epsilon > 0 \\ U^i(Q_F) \frac{D_h(\pi - \epsilon, 0)}{2} \frac{e^{-jks}}{\sqrt{s}}, & \epsilon < 0 \end{cases}$$

where  $s_1, \phi_1$  are the coordinates of the ray diffracted from  $Q_E$ , and

$$(20) \quad U^i(Q_F) = U^i(Q_E) D_h\left(\frac{3\pi}{2}, \phi_1\right) \frac{e^{-jkh}}{\sqrt{h}}.$$

When  $\phi_2 = 0$  and the singly-diffracted ray grazes the vertical surface, the second and fourth terms in the expression for the diffraction coefficient are the same, except for the  $\pm$  sign of the latter. This is also true for the first and third terms. As a result,

$$(21) \quad D_h(\pi - \epsilon, 0) = \frac{-e^{-j\pi/4}}{n\sqrt{2\pi k}} \left\{ \cot\left(\frac{\epsilon}{2n}\right) F[kLa^-(\pi - \epsilon)] \right. \\ \left. + \text{smaller terms which are continuous at } SB(Q_E) \right\}.$$

As  $\epsilon \rightarrow 0$ , it is seen from Eqs. (12), (13), (14) and (15) that

$$(22) \quad D_h(\pi - \epsilon, 0) = -\sqrt{\frac{hs}{s+h}} \operatorname{sgn} \epsilon;$$

furthermore,

$$(23) \quad s_1 = h + s.$$

Substituting Eqs. (22) and (23) into Eq. (19) and making use of Eq. (20), it is seen that the total diffracted field is continuous at the boundary  $SB(Q_E)$ .

As we have already noted, in the case of a soft boundary the field of an incident-ray grazing the surface vanishes, the edge-diffracted field is then proportional to the normal derivative of the incident field at the edge. The proportionality factor is a diffraction coefficient  $D'$  given by Karp and Keller [8]. Thus, for the case of Dirichlet problem, the doubly-diffracted field must be replaced by

$$(24) \quad U^d(Q_E, Q_F) = \frac{\partial U^i(Q_F)}{\partial n} \frac{D'(\phi_2, 0)}{2} \frac{e^{-jks}}{\sqrt{s}}$$

where

$$(25) \quad D'(\phi_2, 0) = \frac{1}{jk} \frac{\partial}{\partial \phi_1} D_s(\phi_2, 0)$$

The derivative  $\partial U(Q_F)/\partial n$  is taken with respect to the normal to the surface  $Q_F Q_F$ . This contribution is weak in comparison with that of the singly-diffracted rays; the contribution of the former is of order  $(1/k^2)$ , whereas that of the latter is of order  $(1/\sqrt{k})$ . In calculating the field diffracted from the soft cylinder, it was found that the field of the doubly-diffracted rays did not contribute significantly, so the contribution from these rays can be omitted in this case.

Let us now turn to the diffraction by a rectangular cylinder illuminated by a line source. Depending on the location of the line source, the whole domain surrounded by the cylinder will be divided into regions by the various shadow boundaries and the reflection boundaries. Each of these boundaries is labeled to indicate how it originates. For example, referring to Fig. 4, the notation, SB means the shadow boundary of the incident geometrical optics field  $U^i(P)$ , RB(A-B) is the shadow boundary of the geometrical optics field  $U^r(A-B)$  reflected from the surface A-B, SB(A) is the shadow boundary of the singly-diffracted  $U^d(A)$ , which emanates from the edge A, and SB(A,B) is the shadow boundary of the doubly-diffracted field  $U^d(A,B)$  which emanates from the edge B. The shadow boundary of the reflected field is referred to simply as the reflection boundary.

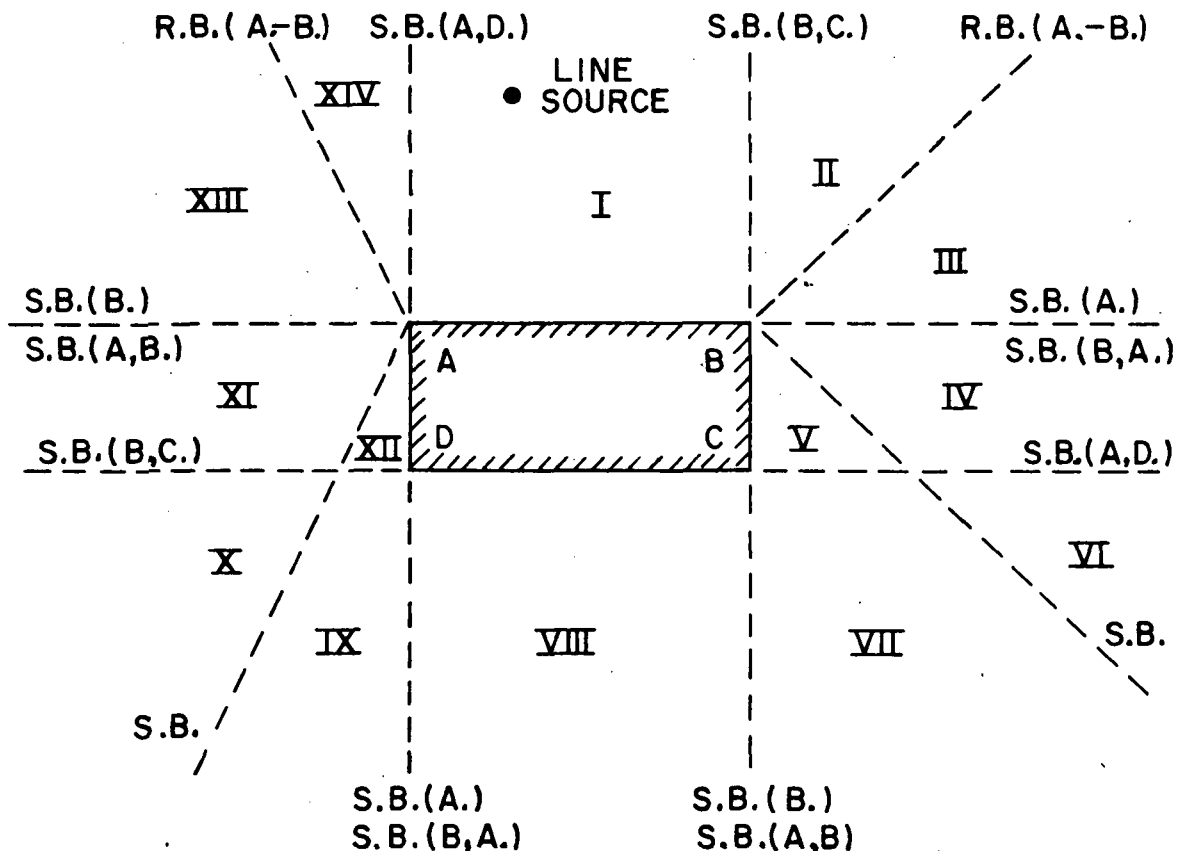


Fig. 4. Shadow and reflection boundaries of the GTD fields.

REGION FIELD	I	II	III	IV	V	VI	VII	VIII	IX	X	XI	XII	XIII	XIV
$\mu^i$	✓	✓	✓	✓		✓				✓	✓		✓	✓
$\mu^r(A-B)$	✓	✓												✓
$\mu^d(A)$	✓	✓	✓						✓	✓	✓	✓	✓	✓
$\mu^d(B)$	✓	✓	✓	✓	✓	✓	✓						✓	✓
$\mu^d(A,B)$	✓	✓	✓	✓	✓	✓	✓						✓	✓
$\mu^d(B,A)$	✓	✓	✓						✓	✓	✓	✓	✓	✓
$\mu^d(A,D)$						✓	✓	✓	✓	✓	✓	✓	✓	✓
$\mu^d(B,C)$		✓	✓	✓	✓	✓	✓	✓	✓	✓				

A CHECK (✓) MEANS THE FIELD IS NON-VANISHING IN THE REGION

TABLE I

In what follows we may locate the line source in the upper left hand quadrant of the space surrounding the cylinder, without loss of generality. Three cases will be considered.

- 1) First, the line source is located directly above the cylinder. The whole domain around the cylinder is divided into 14 regions as shown in Fig. 4. Table I shows the regions covered by each type of ray. To demonstrate the use of the table, let us consider an observation point P in region IX. Examining the column under region IX of Table I, one finds checks(✓) for  $U^d(A)$ ,  $U^d(B,A)$ ,  $U^d(A,D)$ , and  $U^d(B,C)$ . Thus the total field at P is equal to  $U^t(P) = U^d(A) + U^d(B,A) + U^d(A,D) + U^d(B,C)$ .
- 2) The line source is located to the upper left of the cylinder as shown in Fig. 5. In this case there are 18 regions. Table II shows the regions where a particular ray exists and its field makes a non-vanishing contribution.
- 3) Line source at grazing incidence. Let the line source be located in the plane which contains the A-D side of the rectangular cylinder as shown in Fig. 6. This case is of special interest because the trailing edge D lies in the shadow of the leading edge A. Also, it lies on the shadow boundary of the direct geometrical optics field. The behavior of the field at the boundary DP must be treated separately, see Appendix I. As before, the domain surrounding the cylinder is divided into regions as shown in Fig. 6 and Table III gives the regions covered by the individual rays.

Recall that one or more of the various field components is discontinuous at each boundary shown in Figs. 4, 5 and 6 but that all except the discontinuities in the doubly diffracted fields are compensated; e.g., the discontinuities in the geometrical optics field are compensated by the field of the singly-diffracted rays and the discontinuities in the field of the singly-diffracted rays are compensated by the fields of the doubly-diffracted rays.

As a final step in the analysis, the fields of the individual line sources are superimposed to give the field of a linear array of line sources radiating in the presence of the cylinder, see Fig. 7. A computer program has been written to calculate the incident, total and scattered fields once the linear array is specified. Unlike its earlier definition for geometrical optics, the term incident field used here means the field of the array in the absence of the cylinder, and the scattered field is simply the difference between the total field and this incident field. The versatility of such a program is evident; the scattering from the cylinder for a wide variety of illuminations can be studied, and the radiation from antennas in the presence of the rectangular cylinder also can be studied. As a matter of fact, the program



was written originally so that the linear array of line sources, when densely packed, closely approximates the field of an aperture antenna of finite width  $W$ . The aperture antenna (more precisely its axis) is directed toward a point  $Q$  on the surface of the rectangular cylinder as shown in Fig. 7. A description of the aperture radiation in terms of an array of discrete line sources is discussed in the following paragraphs.

The aperture distribution may be approximated by a discrete array of line sources which are properly weighted in amplitude and phase. The width of the aperture denoted by  $W$ , is divided into  $2M$  segments; ( $M$  = integer). The line sources are positioned at the ends of these segments, which introduces  $2M + 1$  line sources. In approximating a continuous distribution, the number  $M$  is selected so that  $2M + 1 \geq 10 W/\lambda$ , where  $\lambda$  = free space radiated wavelength.

Three types of line sources are available in this program:

- Type I            An electric current line source
- Type II          A magnetic current line source
- Type III        A magnetic current moment line source.

As described earlier, the electric current line source radiates an omnidirectional electric field which is parallel to the edge of the rectangular cylinder, and the magnetic current line source radiates an omnidirectional magnetic field which is parallel to the edge of the rectangular cylinder. The magnetic current moment line source consists of a continuous array of magnetic current moments directed perpendicular to the line of the array and parallel to the aperture in question. This line source radiates an electric field parallel to the edge of the cylinder; however, the field has a pattern,  $|\cos \theta|$ , where  $\theta$  is shown in Fig. 7. The strength of these magnetic type line sources is determined from the equivalent magnetic surface currents in the aperture.  $\vec{K}_s = \vec{E} \times \hat{n}$ , where  $\vec{E}$  is the electric field distribution in the aperture (assumed known) and  $\hat{n}$  is the outward normal to the aperture.

The field of the two-dimensional aperture can be adequately represented in the forward direction by a densely-packed array of type II and type III line sources, but such an array fails to approximate the field adequately at aspects behind the aperture. This limitation is particularly troublesome when calculating the total field. To overcome this difficulty an obliquity factor has been included in the program which multiplies the pattern of each line source. The obliquity factor is  $f(\theta) = \cos^n \theta/2$ , where  $n = 0, \frac{1}{2}, 1, 2$ . When  $n = 0$ , the obliquity factor is unity so that the array radiates symmetrically with respect to the axis of its elements. The case  $n = 2$  occurs naturally in the description of the radiation fields of aperture antennas via the Kirchhoff-Huygen's approximation (for the forward region). The cases  $n = \frac{1}{2}$ , and  $n = 1$  are added so that the  $n$  which best approximates the measured aperture pattern may be used. It is evident that the obliquity factor results in a pattern null in the direction directly behind the aperture at  $\theta = \pi$ . In most practical cases, there is no such null in the backward direction.

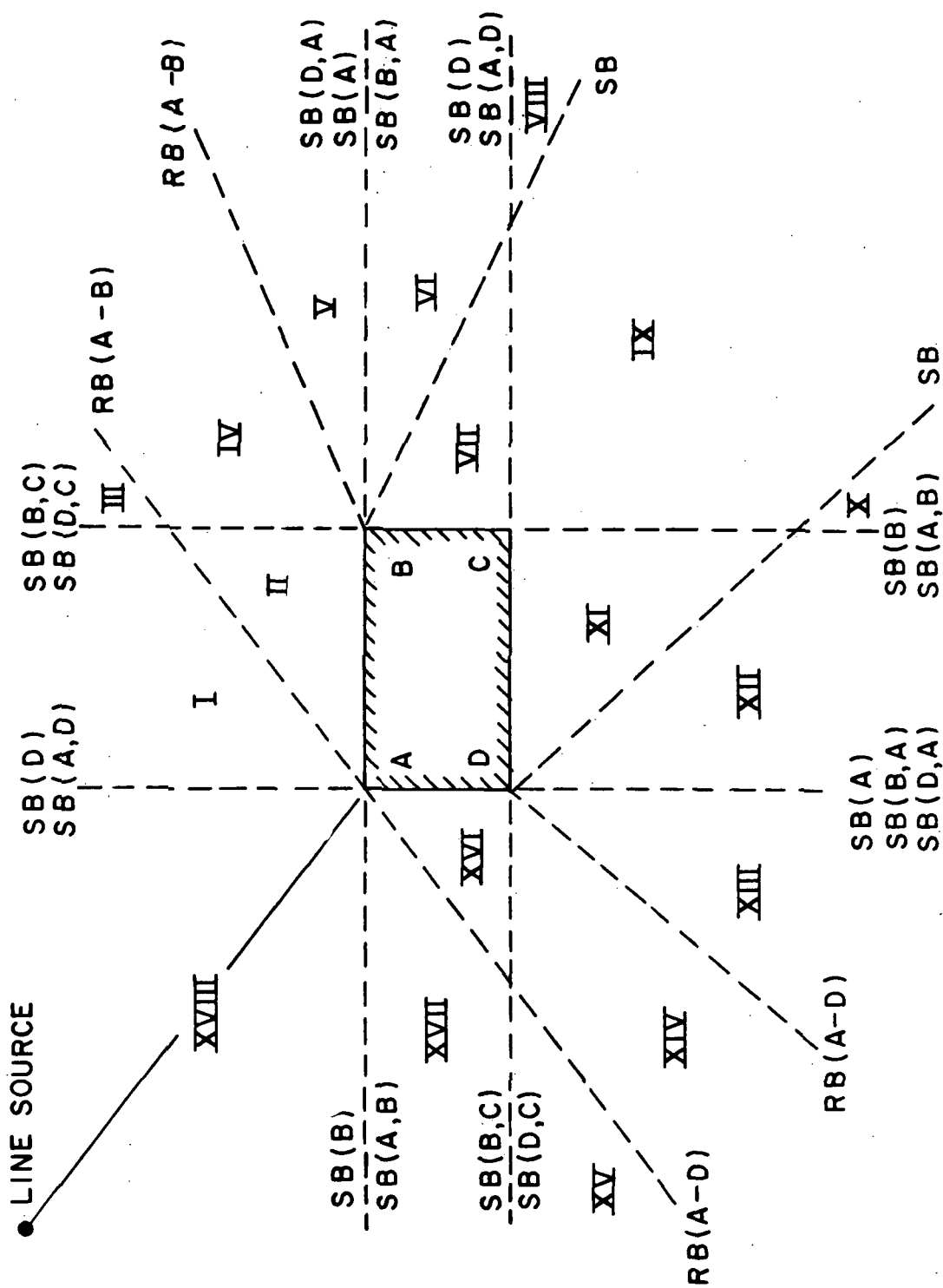


Fig. 5. Shadow and reflection boundaries of the GTD fields.

REGION FIELD	I	II	III	IV	V	VI	VII	VIII	IX	X	XI	XII	XIII	XIV	XV	XVI	XVII	XVIII
$\mu^i$	✓	✓	✓	✓	✓	✓		✓		✓		✓	✓	✓	✓	✓	✓	✓
$\mu^r(A-B)$		✓		✓														
$\mu^r(A-D)$														✓		✓		
$\mu^d(A)$	✓	✓	✓	✓	✓								✓	✓	✓	✓	✓	✓
$\mu^d(B)$	✓	✓	✓	✓	✓	✓	✓	✓	✓	✓								✓
$\mu^d(D)$								✓	✓	✓	✓	✓	✓	✓	✓	✓	✓	✓
$\mu^d(A,B)$	✓	✓	✓	✓	✓	✓	✓	✓	✓	✓								✓
$\mu^d(B,A)$	✓	✓	✓	✓	✓								✓	✓	✓	✓	✓	✓
$\mu^d(A,D)$								✓	✓	✓	✓	✓	✓	✓	✓	✓	✓	✓
$\mu^d(D,A)$	✓	✓	✓	✓	✓								✓	✓	✓	✓	✓	✓
$\mu^d(B,C)$			✓	✓	✓	✓	✓	✓	✓	✓	✓	✓	✓	✓	✓	✓		
$\mu^d(D,C)$			✓	✓	✓	✓	✓	✓	✓	✓	✓	✓	✓	✓	✓	✓		

TABLE II

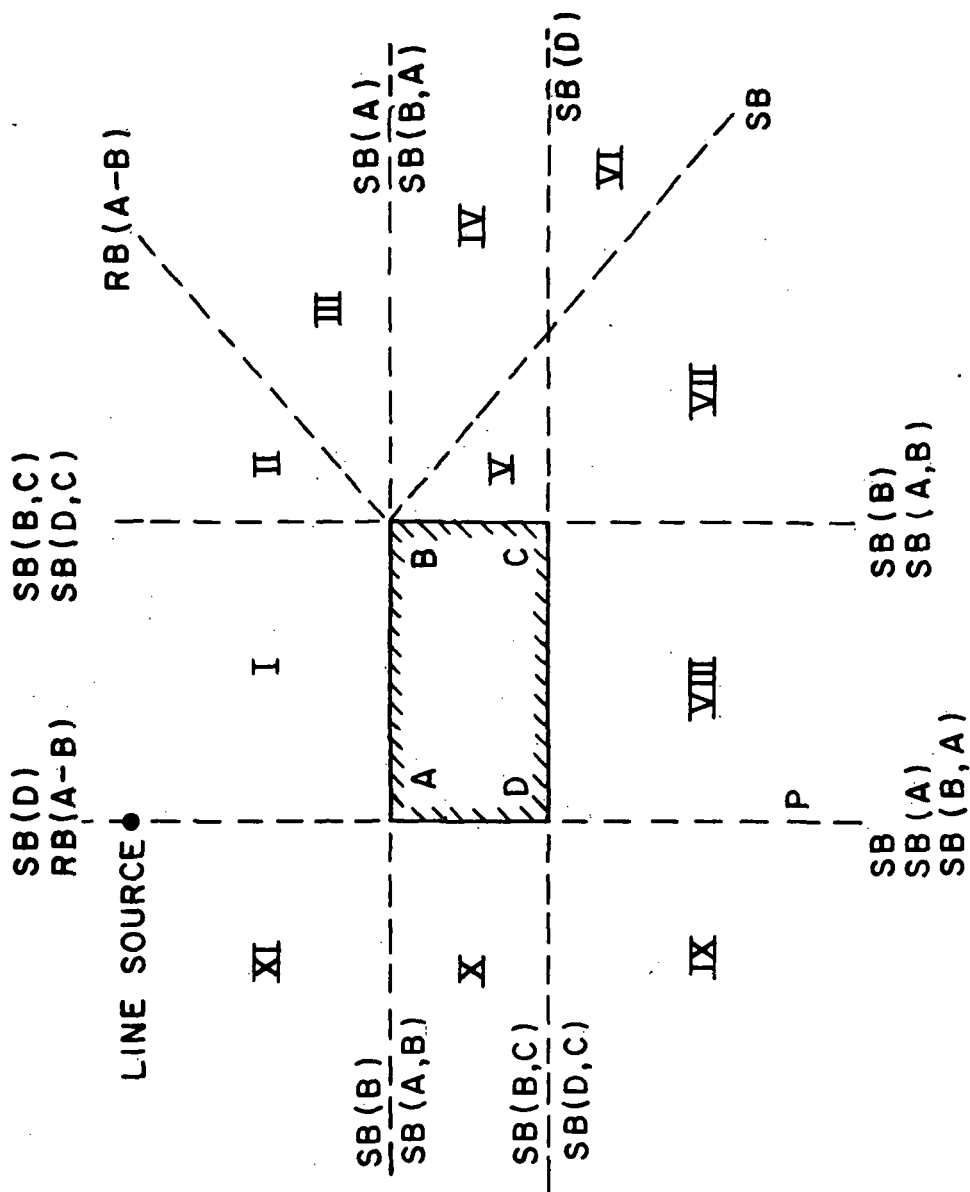


Fig. 6. Shadow and reflection boundaries of the GTD fields.

REGION FIELD	I	II	III	IV	V	VI	VII	VIII	IX	X	XI
$\mu^i(p)$	✓	✓	✓	✓		✓			✓	✓	✓
$\mu^r(A-B)$	✓	✓									
$\mu^d(A)$	✓	✓	✓						✓	✓	✓
$\mu^d(B)$	✓	✓	✓	✓	✓	✓	✓				✓
* $\mu^d(D)$						✓	✓	✓	✓	✓	✓
$\mu^d(A,B)$	✓	✓	✓	✓	✓	✓	✓				✓
$\mu^d(B,A)$	✓	✓	✓						✓	✓	✓
$\mu^d(B,C)$		✓	✓	✓	✓	✓	✓	✓	✓		
$\mu^d(D,C)$		✓	✓	✓	✓	✓	✓	✓	✓		

\* SEE APPENDIX I

TABLE III

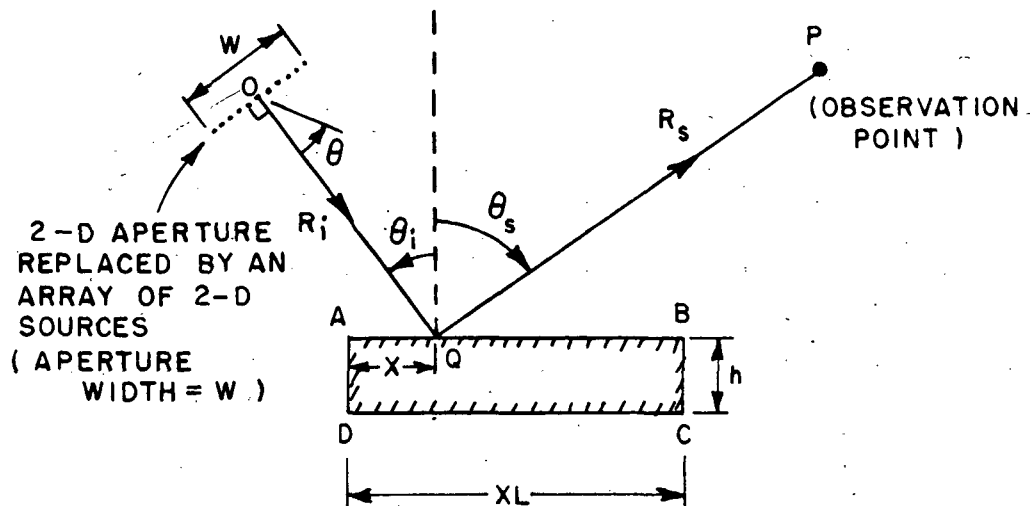


Fig. 7. An array of line source in the presence of the rectangular cylinder.

On the other hand, the pattern in the forward region is quite satisfactory when the obliquity factor is included, and as one moves away from the forward region, the pattern drops to a level where the differences between the simulated and measured patterns are unimportant when computing the total field surrounding the rectangular cylinder.

The scattered, and the total fields are computed as a function of  $\theta_s$  ( $-\pi \leq \theta_s \leq \pi$ ) at a range  $R_s$ . The incident field pattern on the other hand is available for a phase reference at the center of the array (aperture) at  $O$  in Fig. 7 and computed at a range measured from  $O$ , as well as for a phase reference at  $Q$  with a range  $R_s$  (just as for the scattered and the total fields).

The input and output variables for the computer program are described in Appendix II, and the listing of the computer program is given. Also, a sample case is treated in this appendix to illustrate the use of the program.

### III. NUMERICAL RESULTS

To assess the accuracy of the GTD solution described in the preceding section, it was applied to several simple examples, where the rectangular cylinder is illuminated by either an electric or magnetic current line source. Far-zone patterns for the total field are calculated by this method and also from numerical solutions of the pertinent integral equation\*. The cylinders are square with a side length of 1.6

\*The computer programs for the integral equation solutions were provided by Prof. J.H. Richmond of the ElectroScience Laboratory.

wavelength, and in each case the line source illuminates the cylinder from a distance of 0.8 wavelength. These small distances provide a stringent test of our GTD solution; also they give us an opportunity to examine the accuracy of the new scalar diffraction coefficients in a situation where the edges are illuminated by curved wavefronts and where the transition regions are relatively broad. The pattern calculated from the integral equation solution must be considered more accurate for the small dimensions chosen for these examples, since the integral equation method is convergent whereas the GTD solution is an asymptotic approximation.

Patterns for magnetic current line source excitation (hard boundary case) are given in Figs. 8, 9 and 10, where the line source is positioned on the diagonal of the square cylinder, on the centerline directly above the cylinder, and at a point of glancing incidence on one of its surfaces. The agreement between the patterns calculated by the GTD and the integral equation method is remarkable - every detail is the same within the limits of graphical accuracy. The corresponding patterns for electric current line source excitation (soft boundary case) are presented in Figs. 11, 12 and 13. Again there is excellent agreement between the two pattern calculations, except in the vicinity region of forward scatter in Figs. 12 and 13. Note that the level of the patterns is very low in these regions, so that small errors in the solution become significant. We hope to look into the reason for these differences at a later time.

The numerical examples considered here confirm the accuracy and applicability of our GTD solution; this is further demonstrated by an example treated in Appendix II. As the size of the cylinder and the distance between the edges of the cylinder and the source (or sources) increases in terms of a wavelength, one can expect the accuracy of the GTD solution to increase, because it is an asymptotic approximation where  $k = 2\pi/\lambda$  is a large parameter.

In the case of magnetic current line source excitation there is little evidence of shadowing in the forward direction by the small square cylinder; however, there is distinct evidence of shadowing in the case of electric current line source excitation, where the total electric field is parallel to the cylinder and must vanish at its surface. One should expect this.

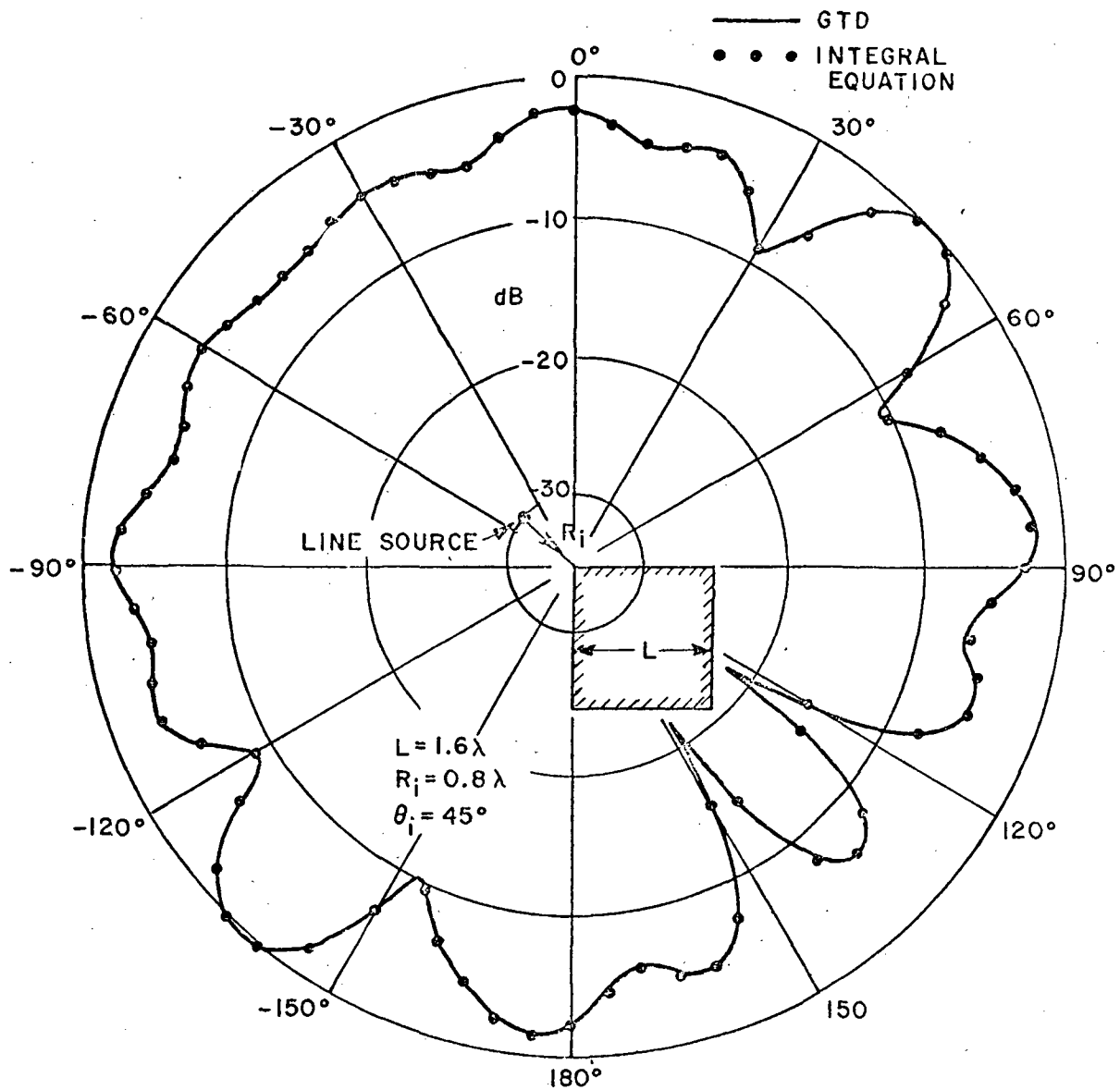


Fig. 8. Pattern of a magnetic current line source in the presence of a rectangular cylinder.



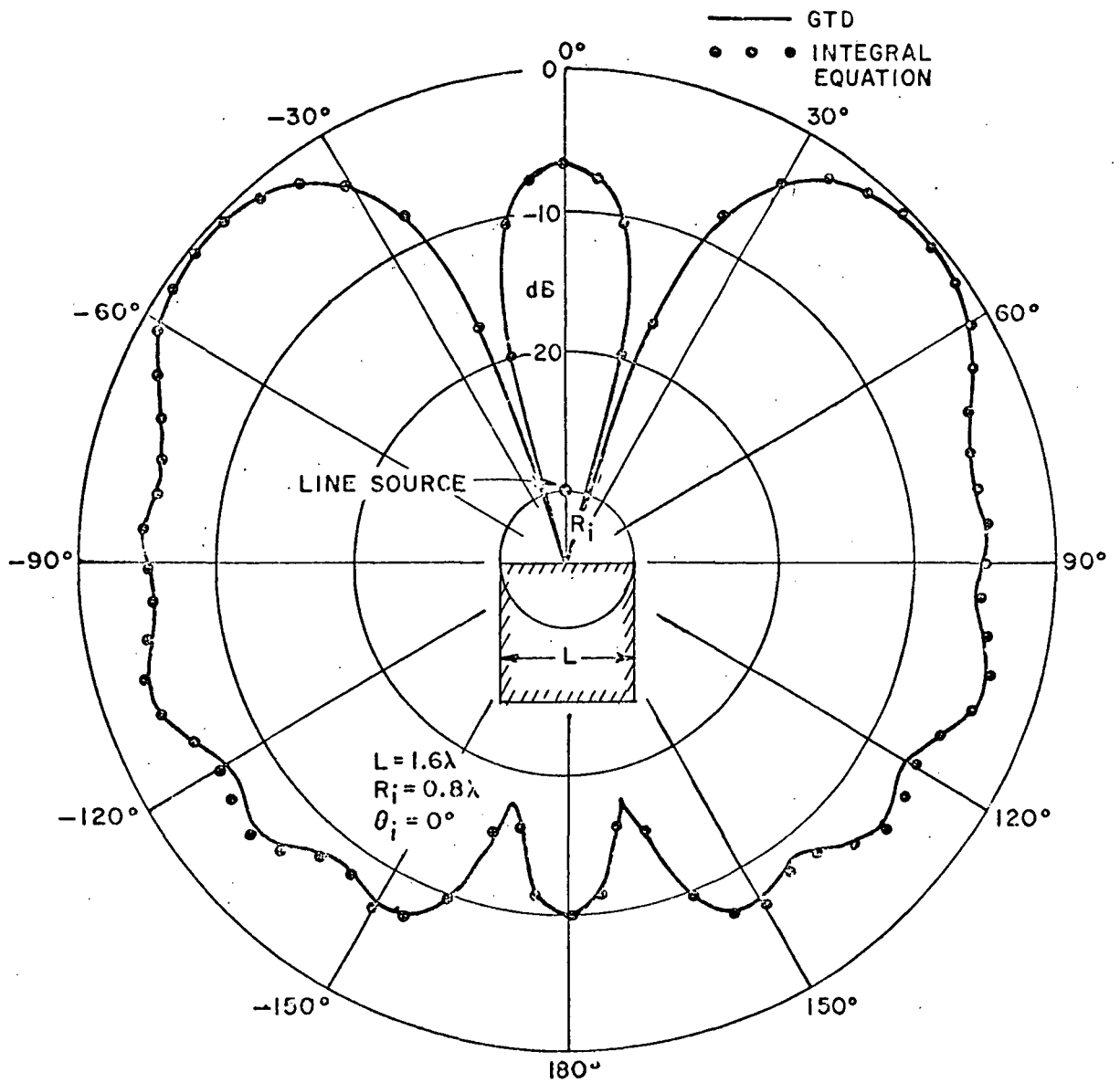


Fig. 9. Pattern of a magnetic current line source in the presence of a rectangular cylinder.

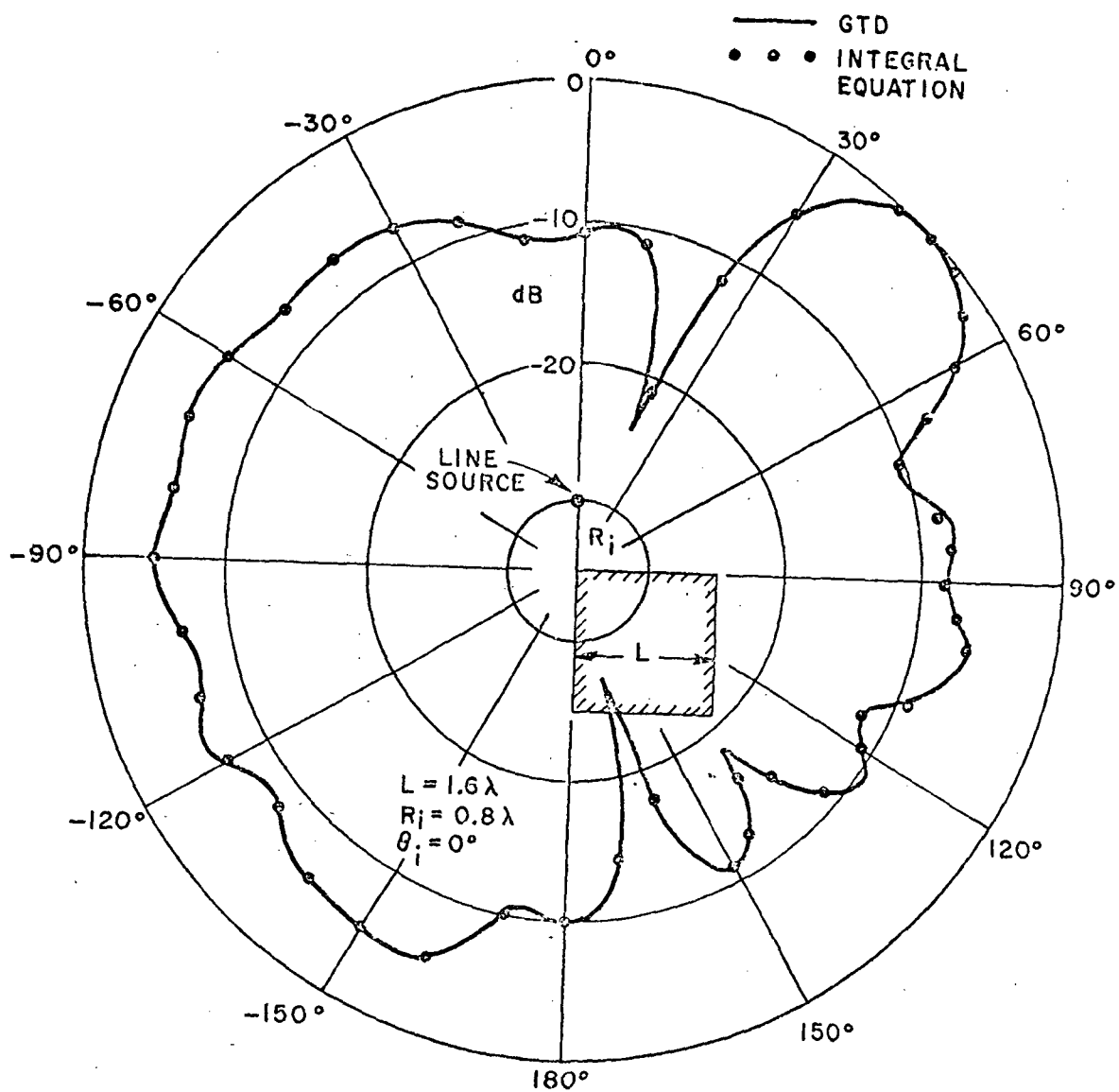


Fig. 10. Pattern of a magnetic current line source in the presence of a rectangular cylinder.

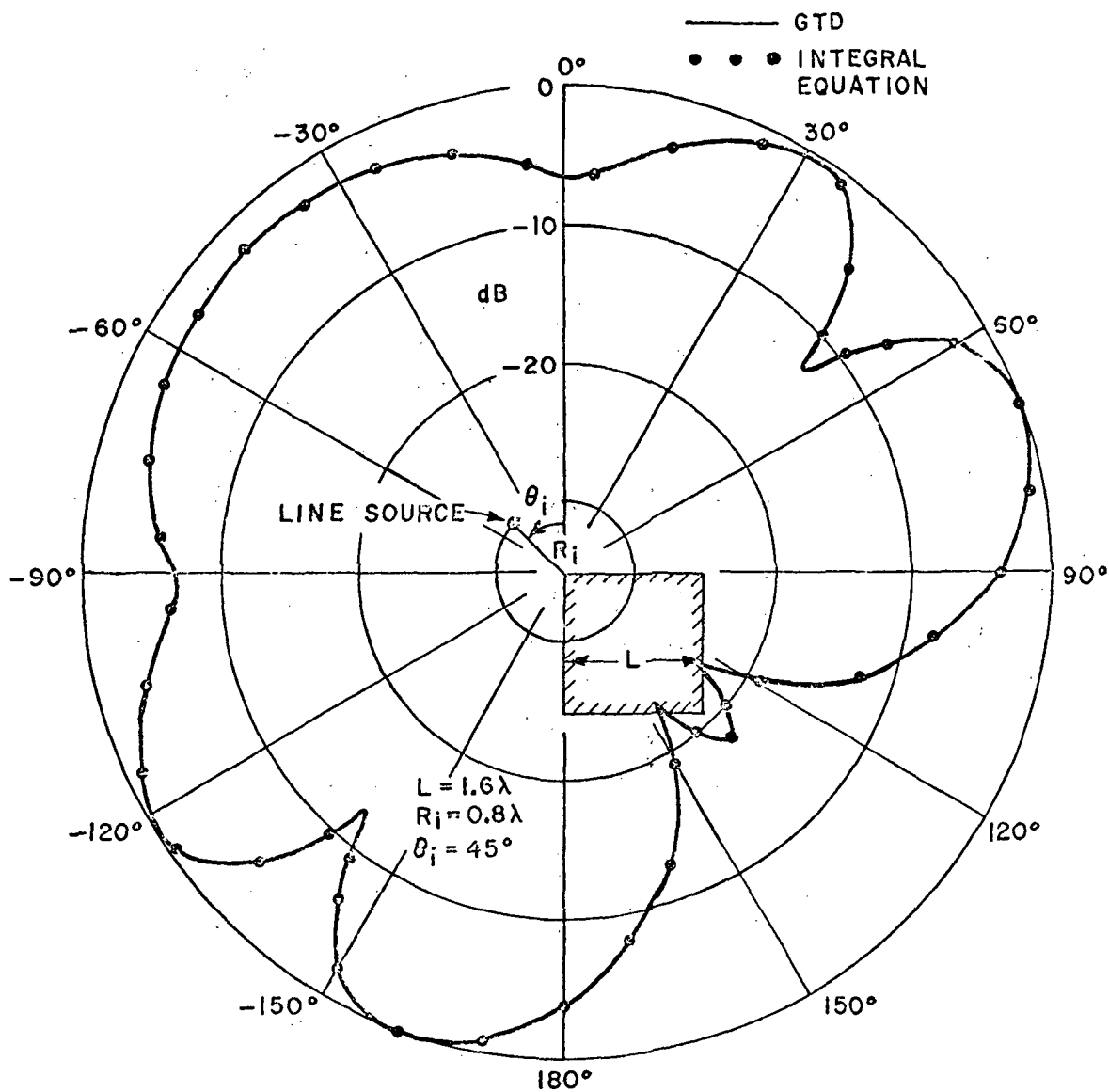


Fig. 11. Pattern of an electric current line source in the presence of a rectangular cylinder.

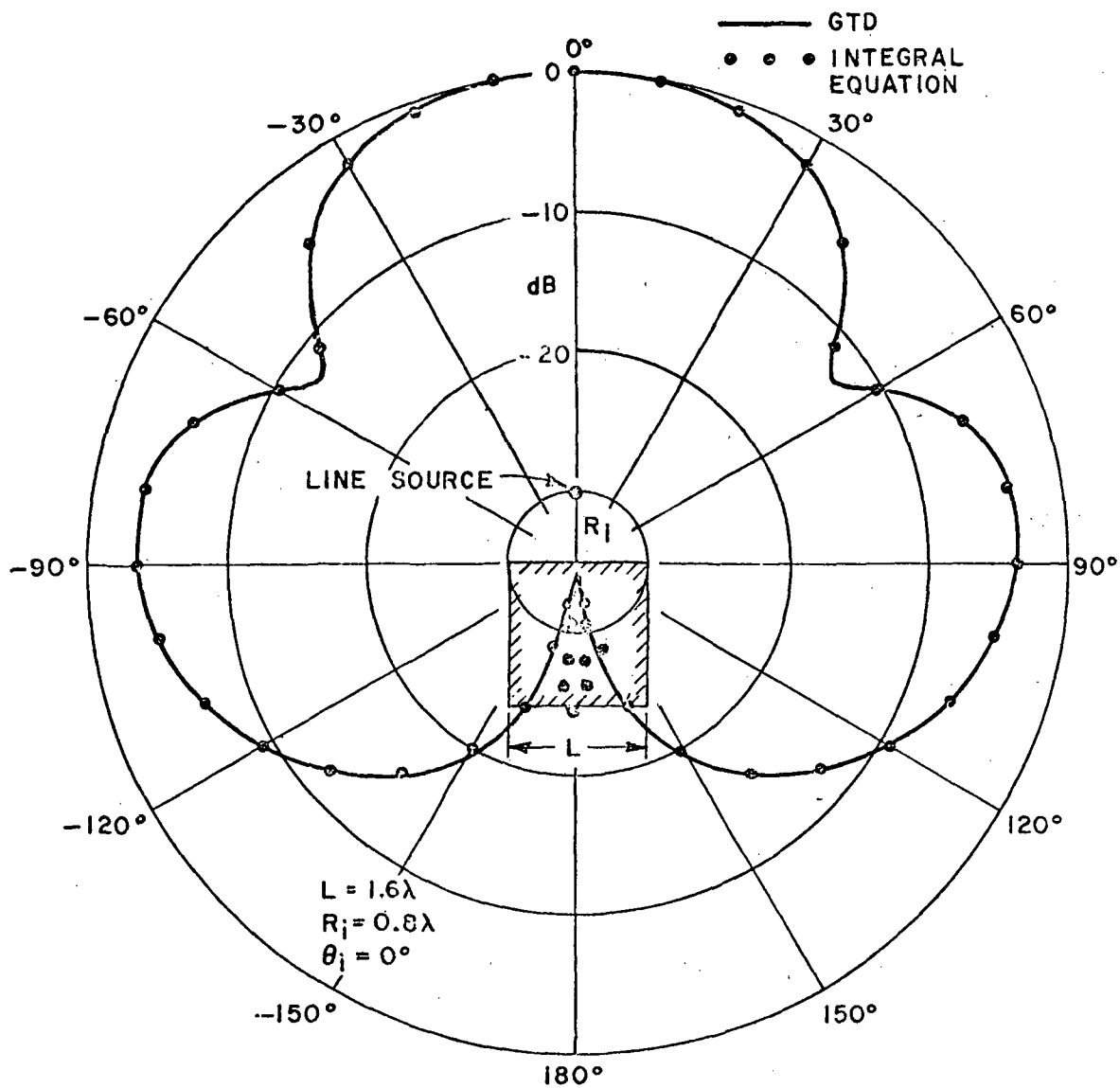


Fig. 12. Pattern of an electric current line source in the presence of a rectangular cylinder.

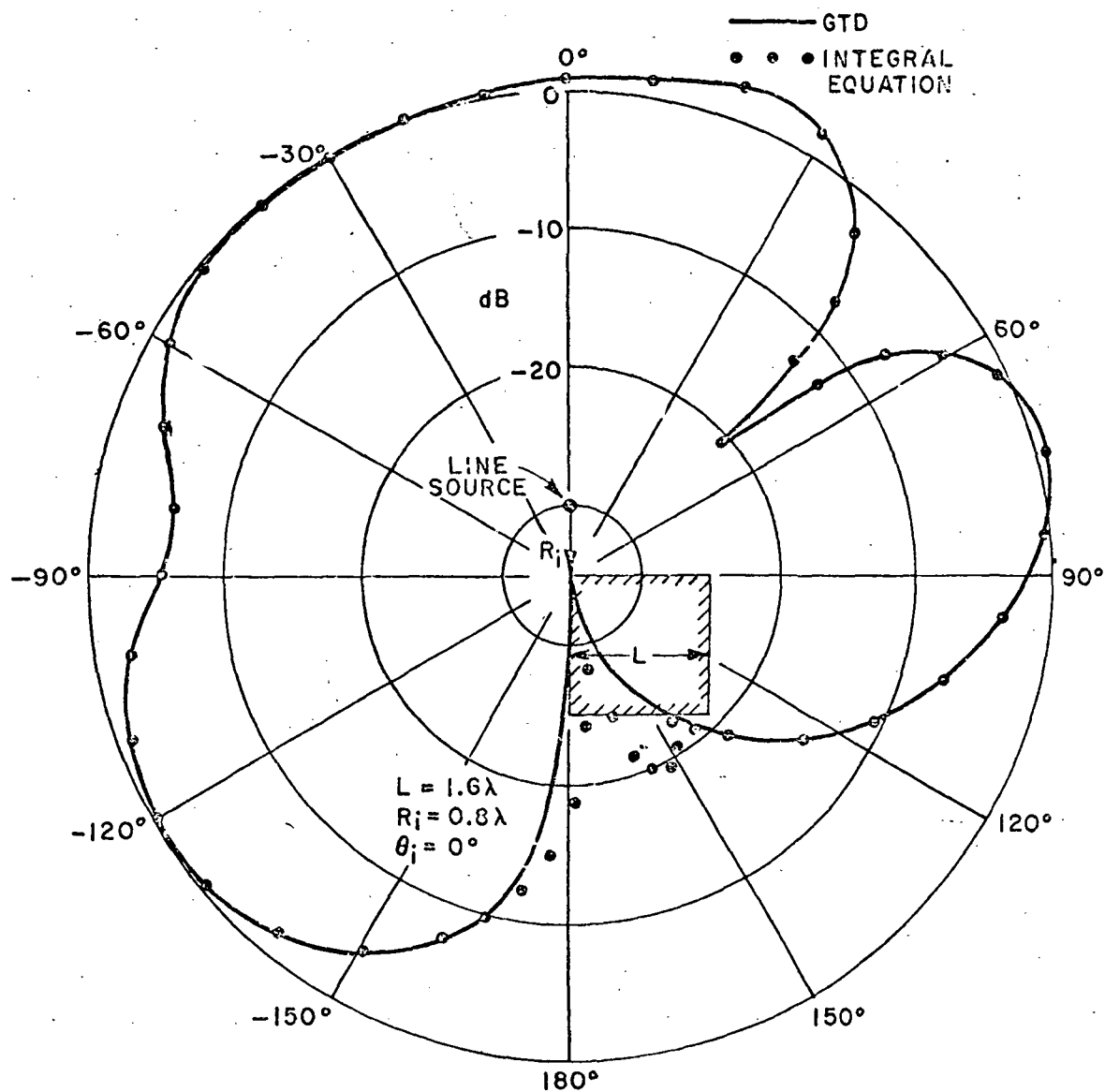


Fig. 13. Pattern of an electric current line source in the presence of a rectangular cylinder.

#### IV. CONCLUSIONS

The GTD has been applied to calculate the radiation from a perfectly-conducting rectangular cylinder in the presence of a linear array of line sources, which may be of the electric current, magnetic current or magnetic current moment type. When densely packed, these sources may be used to approximate the radiation from an aperture. To insure good accuracy in the fields calculated from the solution described here, the separation of source and field points from the edges of the cylinder and the separation of the edges from each other should be not less than 0.7 wavelength. However, for far-zone pattern calculations, the line sources can be only a few tenth of a wavelength from the nearest edge.

The use of new scalar diffraction coefficients valid in the transition regions makes it possible to calculate continuous patterns in the region surrounding the cylinder away from its edges. Radiation patterns calculated from this solution and from an integral equation solution are found to be in excellent agreement for a number of stringent test cases. This demonstrates the utility and accuracy of the new diffraction coefficients and the overall accuracy of GTD as it has been applied to this problem.

## APPENDIX I

THE FIELD AT THE SHADOW BOUNDARY OF A  
THICK SCREEN FOR GRAZING INCIDENCE

In this appendix we derive an expression for the field near the shadow boundary of a thick, perfectly conducting screen illuminated by a line source at grazing incidence, as shown in Fig. 14. The solution near the shadow boundary in the forward direction is of interest. In the following development we employ Eqs. (5) through (10) in the text, the subscript  $h$  on the hard scalar diffraction coefficient has been omitted, and it is convenient to use the function

$$(A-1) \quad f(x) = \frac{e^{-jkx}}{\sqrt{x}}$$

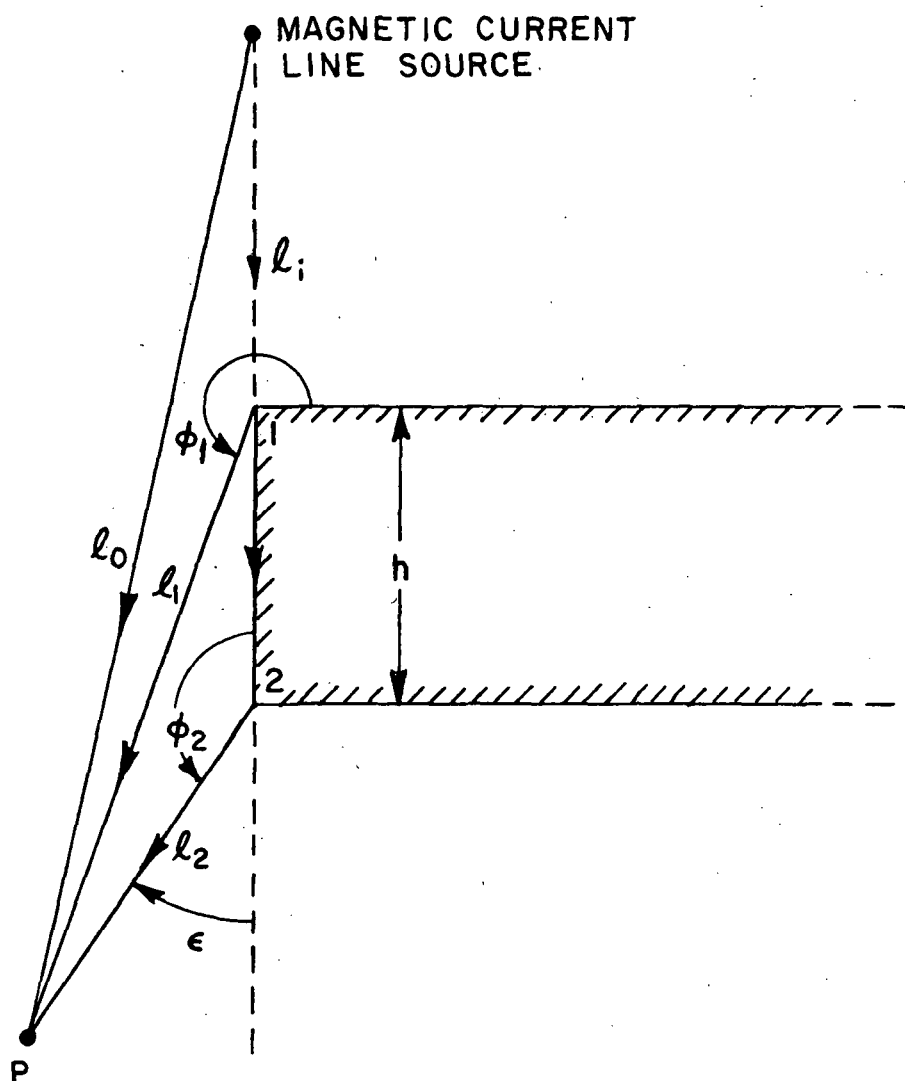


Fig. 14. Shadow boundary of a thick screen for grazing incidence.

Let the strength of the line source be such that the incident field at P is

$$(A-2) \quad U^i(P) = f(\ell_0)$$

The total field at P is the sum of the incident field plus the field of the ray singly-diffracted from edge 1 and the field of the ray doubly-diffracted from edge 2. In the illuminated region,  $\epsilon > 0$ ,

$$(A-3a) \quad U(P) = f(\ell_0) + f(\ell_i) D(\phi_1, \frac{\pi}{2}; L_1) f(\ell_1) + \frac{1}{2} U^i(2) D(\phi_2, 0, L) f(\ell_2)$$

In the shadow region,  $\epsilon < 0$ ,

$$(A-3b) \quad U(P) = \frac{1}{2} U^i(2) D(\phi_2, 0, L) f(\ell_2)$$

Here,

$$(A-4a) \quad \phi_2 = \pi - \epsilon$$

$$(A-4b) \quad L_1 = \frac{\ell_i \ell_1}{\ell_i + \ell_1}$$

$$(A-4c) \quad U^i(2) = f(\ell_i + h) + f(\ell_i) \left[ -\frac{2}{3} e^{-j\pi/4} \cot\left(\frac{2\pi}{3}\right) F(2kL'_1) \right] f(h)$$

in which

$$(A-4d) \quad L'_1 = \frac{\ell_i h}{\ell_i + h}$$

Thus for  $\epsilon > 0$ ,

$$(A-5a) \quad U(P) = f(\ell_0) + f(\ell_i) D(\phi_1, 0; L_1) f(\ell_1) + \frac{1}{2} f(\ell_i + h) D(\phi_2, 0; L_2) f(\ell_2) \\ + \frac{1}{2} f(\ell_i) f(h) \left[ -\frac{2}{3} e^{-j\pi/4} \cot\left(\frac{2\pi}{3}\right) F(2kL'_1) \right] D(\phi_2, 0, L) f(\ell_2)$$



and for  $\epsilon < 0$ ,

$$(A-5b) \quad U(P) = \frac{1}{2} f(\ell_1 + h) D(\phi_2, 0, L_2) f(\ell_2) + \frac{1}{2} f(\ell_1) f(h) \cdot \\ \cdot \left[ -\frac{2}{3} e^{-j\pi/4} \cot\left(\frac{2\pi}{3}\right) F(2kL_1) \right] D(\phi_2, 0, \bar{L}) f(\ell_2) \quad ,$$

where

$$(A-6) \quad L_2 = \frac{(\ell_1 + h) \ell_2}{\ell_1 + h + \ell_2}$$

and  $\bar{L}$  is a distance parameter determined by the wavefront curvature of the field incident on edge 2 which has been singly-diffracted from edge 1. Since edge 2 is in the transition region of this field, the curvature of this wavefront is not simply that of a cylindrical wave emanating from edge 1; i.e.,  $\bar{L} \neq h \ell_2 / (h + \ell_2)$ . We will determine  $\bar{L}$  by requiring  $U(P)$  to be continuous at the shadow boundary.

As  $\epsilon \rightarrow 0$ ,

$$(A-7) \quad D(\phi_2, 0, L_2) = \frac{-e^{-j\pi/4}}{n\sqrt{2\pi k}} \left(\frac{2n}{\epsilon}\right) \sqrt{\frac{\pi k L_2}{2}} |\epsilon| e^{j\pi/4} \\ = -\sqrt{L_2} \operatorname{sgn} \epsilon \quad .$$

In a similar manner,

$$(A-8) \quad D(\phi_2, 0, \bar{L}) = -\sqrt{\bar{L}} \operatorname{sgn} \epsilon \quad .$$

Furthermore, as  $\epsilon \rightarrow 0$

$$(A-9) \quad D(\phi_1, 0; L_1) = -\frac{2}{3} e^{-j\pi/4} \cot\left(\frac{2\pi}{3}\right) \frac{F(2kL_1)}{\sqrt{2\pi k}}$$

Substituting Eqs. (A-7), (A-8) and (A-9) into Eqs. (A-5a), (A-5b) and requiring  $U(P)$  to be continuous at the shadow boundary  $\epsilon = 0$ , we see that

$$(A-10) \quad \frac{e^{jk(\ell_1 + \ell_1)}}{\sqrt{\ell_1 \ell_1}} \left\{ -\frac{2}{3} e^{-j\pi/4} \cot\left(\frac{2\pi}{3}\right) \frac{F(2kL_1)}{\sqrt{2\pi k}} \right\} =$$

$$\frac{e^{-jk(\ell_1 + h + \ell_2)}}{\sqrt{\ell_1 h \ell_2}} \left\{ -\frac{2}{3} e^{-j\pi/4} \cot\left(\frac{2\pi}{3}\right) \frac{F(2kL_1')}{\sqrt{2\pi k}} \right\} \sqrt{\bar{L}}$$

where  $h + \ell_2 = \ell_1$  at  $\epsilon = 0$ .

From which

$$(A-11) \quad \bar{L} = \left( \frac{h \ell_2}{h + \ell_2} \right) m$$

with

$$(A-12) \quad m = \left[ \frac{F(2kL_1)}{F(2kL_1')} \right]^2$$

## APPENDIX II

### DESCRIPTION OF THE COMPUTER PROGRAM

#### A. Input Variables

- N : is the number of sources in the array which approximates the aperture distribution. Here  $N = 2M+1$ , where  $M$  is an integer ( $\therefore N$  is an odd integer), and  $M$  has been introduced earlier in section II. The DIMENSION cards at the beginning of the program must be dimensioned as  $N$  or larger.
- TYPE : is a reference parameter. TYPE is set equal to 1.0 when sources of type I (see section II) are used. TYPE is likewise set equal to 2.0 for type II, and is set equal to 3.0 for type III sources, respectively.
- AL : is the aperture width (=  $W$  of Fig. 7).
- AM(I): is the magnitude of the  $I$ th source in the array which approximates a given aperture distribution.
- AP(I): is the phase of the  $I$ th line source in the array (which approximates a given aperture distribution), in RADIANS.
- X : is the point of incidence on the 2-D box and corresponds to  $X$  shown in Fig. 7.
- XL : is the length of the box (corresponding to  $XL$  of Fig. 7).
- H : is the height of the box (it corresponds to  $h$  in Fig. 7).
- RI : is the incident range (corresponding to  $R_i$  in Fig. 7).
- RS : is the scattered range (corresponding to  $R_s$  in Fig. 7).
- THI : is the angle of incidence (corresponding to  $\theta_i$  in Fig. 7).
- XLAMDA: is the transmitted wavelength.

Note that the variables AL, XL, H, X, RI and RS have the same units as XLAMDA.

#### B. Output Variables

- THS : is the angle of scattering (corresponding to  $\theta_s$  in Fig. 7) in degrees.
- ATAL : magnitude of the total field.

DBTAL: magnitude of the total field in dB.

DBSAS: magnitude of the scattered field in dB.

DBGA : incident field with phase center at Q (Fig. 7) as a function of THS, in dB.

PHASE: phase of the total field in degrees.

TH : angular variable corresponding to (Fig. 7), in degrees

DBHA : incident field with phase center at O (Fig. 7) in dB, as a function of TH. Note that DBHA is an output variable in the Subroutine TEST.

C. Instructions for Representing Aperture Field Distribution by a 2-D Line Source Array.

When dealing with the input variables AM(I) and AP(I) for Ith source in the planar array used to approximate a given aperture distribution, the ordering of the array elements is done as follows:

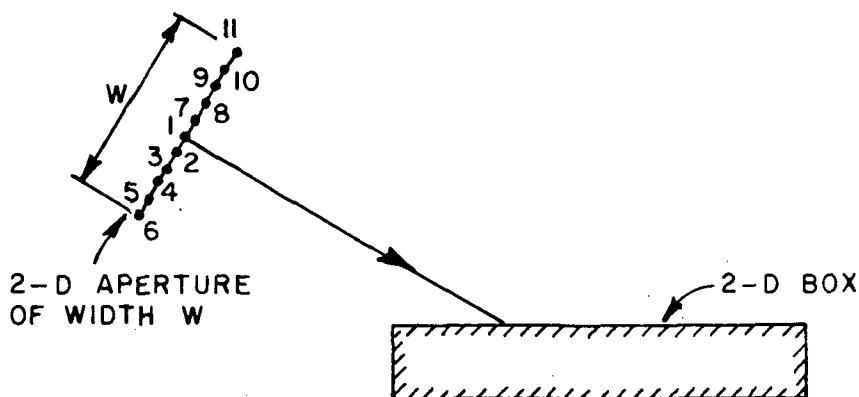


Fig. 15. The ordering arrangement of the line sources used to approximate a given aperture distribution.

Let  $N = 11$ , where  $N$  is the number of line sources approximating a given aperture distribution over the aperture width  $W$ . The ordering arrangement for these sources is indicated in Fig. 15. The source at the center of the aperture is the one for which  $I = 1$ .  $I = 2, 3, 4, 5$  and  $6$  for sources to the right of the one designated by  $I = 1$  (as one views the 2-D box from the aperture center). Similarly,  $I = 7, 8, 9, 10$  and  $11$  for sources to the left of the source at the center (designated by  $I = 1$ ).

Let the aperture distribution (assumed known) be represented by the quantity  $F = |F|e^{i\psi}$  over the aperture.  $|F|$  represents the magnitude of

the field distribution over the width  $W$ , and  $\psi$  represents the phase of the field distribution over the width  $W$ . Hypothetical plots of  $|F|$  and  $\psi$  over the aperture are indicated below:

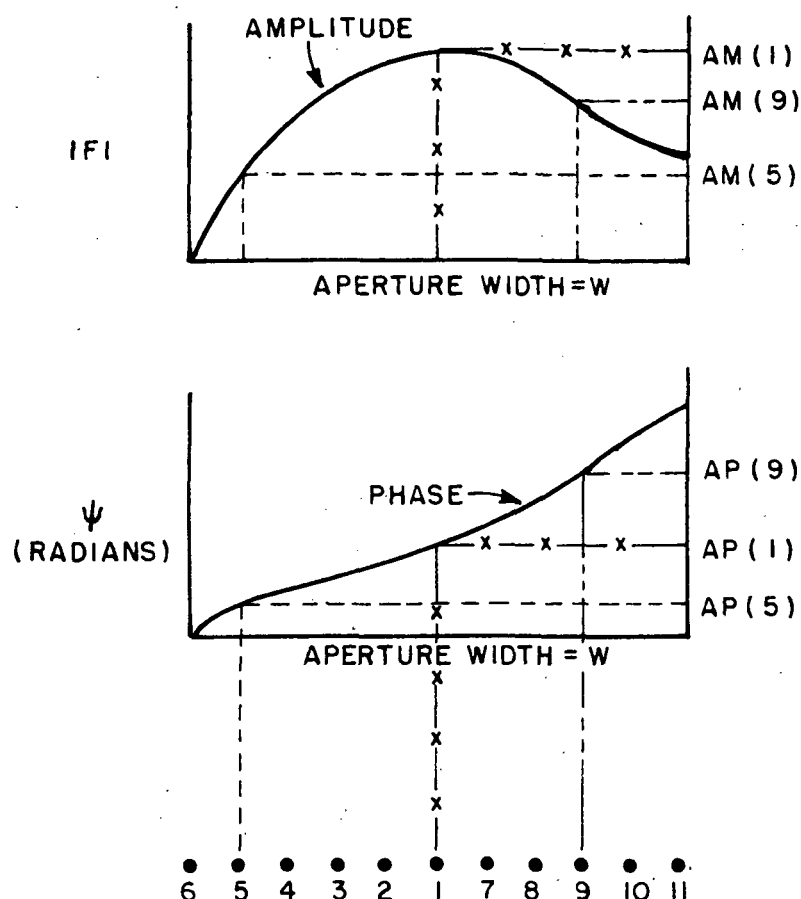


Fig. 16. Field distribution over the aperture.

Fig. 16 clearly indicates the amplitudes and phases of the sources designated by  $I = 1, 5$  and  $9$ . For example, the magnitude of the line source strength corresponding to  $I = 9$  is given by  $AM(9)$ , and its phase is given by  $AP(9)$ . Similarly, one can obtain the amplitudes and phases of all the other line sources. Note that the aperture is divided into  $2M$  segments, where  $M = 5$ . Hence, the number of sources,  $N = 2M + 1 = 11$ .

#### D. Instructions for Using the 'Obliquity Factor'

The fields radiated by apertures are non-symmetrical on either side of the aperture, in most practical cases. The fields radiated by the 2-D line source array discussed above are symmetrical on either side of the planar 2-D array. Thus, an obliquity factor of the type  $\cos^n \theta/2$  (please refer to the discussion in section II) is included for computing the field radiated by each source in the array. The obliquity factor is different for each  $n$ , where  $n = 0, \frac{1}{2}, 1, 2$ . A function statement  $FB(SX)$  computes this obliquity factor for a given value of  $n$ . Specifically, the statement concerning  $FB(SX)$  reads:

$$FB(SX) = ABS(COS(SX/2.0))^{**2.0}$$

and corresponds to an obliquity factor with  $n = 2.0$ . If any other value of  $n$  is desired, the appropriate value must be punched into a new card which replaces the previous one. Note that the value of  $n$  directly follows the  $**$  symbol in the statement.

The obliquity factor  $\cos^n \theta/2$  is plotted as a function of  $\theta$  for different values of  $n$  ( $n = \frac{1}{2}, 1$  and  $2$ ) in Fig. 17. When the pattern of an isotropic source is multiplied by  $\cos^n \theta/2$ , it is evident from the resultant pattern that the obliquity factor serves to control the level of the radiation pattern primarily in the range  $\pi/3 < \theta < 5\pi/3$ . The case  $n = 0$  corresponds to the isotropic case.

#### E. Instructions for Computing the Incident Field

Two incident field patterns are computed, one is for a phase reference at the center of the aperture, and the other is for a phase reference at  $Q$  (see Fig. 7). In the former case, the radiation pattern in dB is designated by DBHA, and is obtained as a function of  $\theta$  (or TH as defined in the computer program). In the latter case, the radiation pattern in dB is designated by DBGA and is obtained as a function of  $\theta_s$  (or THS as defined in the computer program). DBGA is computed at a distance equal to  $R_s$  from  $Q$ . DBHA has been programmed for a range of  $R_i + R_s$  from 0 (center of the aperture as shown in Fig. 7); however, if the user wishes to change the present range for DBHA, only one card in the program deck needs modification. A subroutine designated TEST computes DBHA at a range of  $R_i + R_s$  from 0; the call statement for this subroutine is

CALL TEST (N, AL, RS+RI, A, TYPE)

If a different value of the range is desired, one must replace  $RS+RI$  in the call statement above by a number which equals the desired value for the range. Note that the new range should have the same unit as those of  $\lambda$  (corresponding to XLAMDA in the computer program).

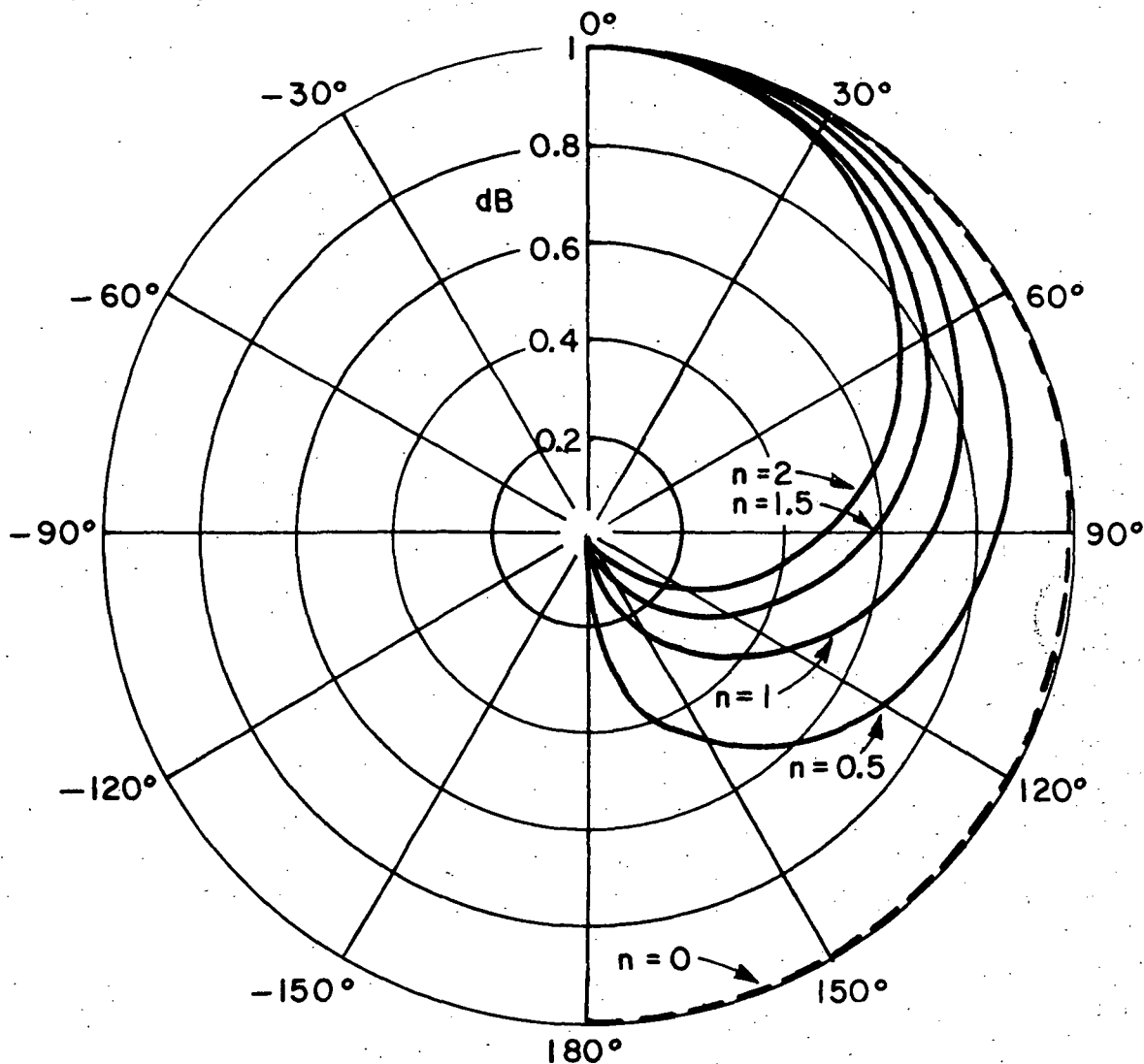


Fig. 17. Patterns of the obliquity factor for different values of  $n$ .

#### F. Sample Programs

In this section, we present a sample case which serves to illustrate the use of our computer program. The example selected involves an array of three magnetic line sources of unit strength which illuminate a rectangular cylinder, as in Fig. 18. We utilize the computer program for calculating the incident field of the array, the field scattered by the 2-D box (rectangular cylinder) and the total field (incident + scattered) surrounding the 2-D box.

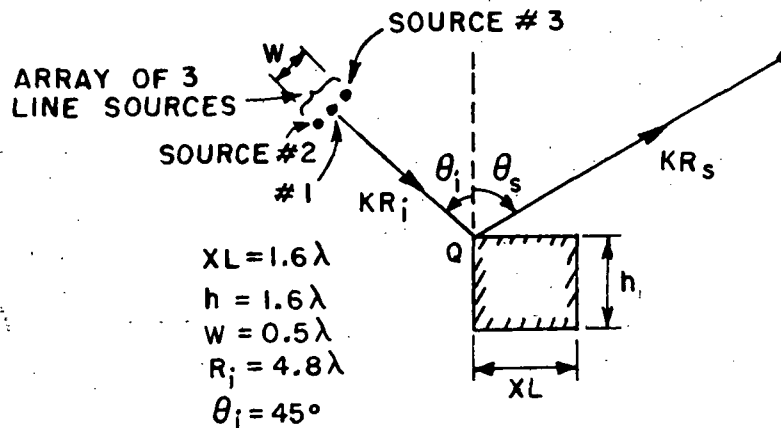


Fig. 18. An array of three line sources in the presence of a square cylinder.

The ordering of the array elements is shown in Fig. 18, where the source at the center is labeled source #1. Note that source #1 corresponds to  $I = 1$ , and sources #2 and #3 correspond to  $I = 2$ , and  $I = 3$ , respectively. For this particular problem,  $AM(1)$ ,  $AM(2)$  and  $AM(3)$  are each equal to 1.0, and  $AP(1)$ ,  $AP(2)$  and  $AP(3)$  are each equal to 0.0, because the line sources are of unit strength and zero phase. An obliquity factor corresponding to  $n = 2$  (i.e., obliquity factor =  $\cos^2 \theta/2$ ) has been incorporated into the program for the incident field pattern, and the incident field pattern corresponding to DBHA (phase reference at source #1) is plotted in Fig. 19. Also included in Fig. 19 is the incident field pattern without the obliquity factor ( $n = 0$  case) for the sake of comparison. The pattern of the scattered field designated by DBSAS, and computed for values of  $\theta_s$  (or THS) which lie in the range  $-180^\circ \leq \theta_s \leq 180^\circ$ , is plotted in Fig. 20. The scattered field obtained by our method is compared against that obtained from a numerical solution to the integral equation for this problem given by J. H. Richmond; these results agree perfectly. Finally, the total field (incident plus scattered, each being phase referenced at  $Q$ ) is also obtained, and is designated by DBTAL. DBTAL is computed as a function of  $\theta_s$  (THS in the program) and the results are indicated in Fig. 21 by a dashed curve. The solid curve is added for the sake of comparison; it corresponds to the total field when the incident field has no obliquity factor in it.



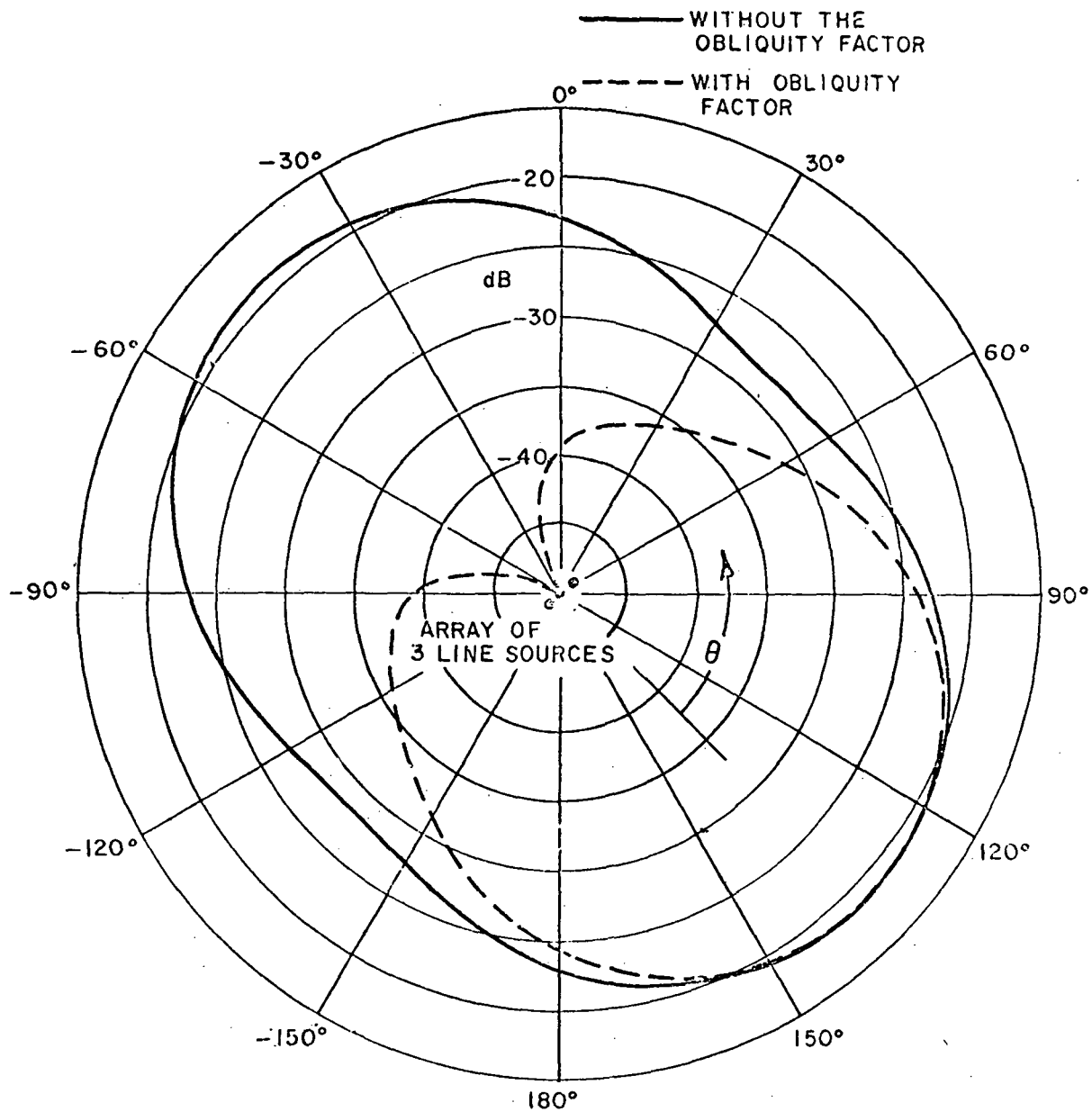


Fig. 19. Patterns of an array of three magnetic line sources of equal strength, with and without the obliquity factor.

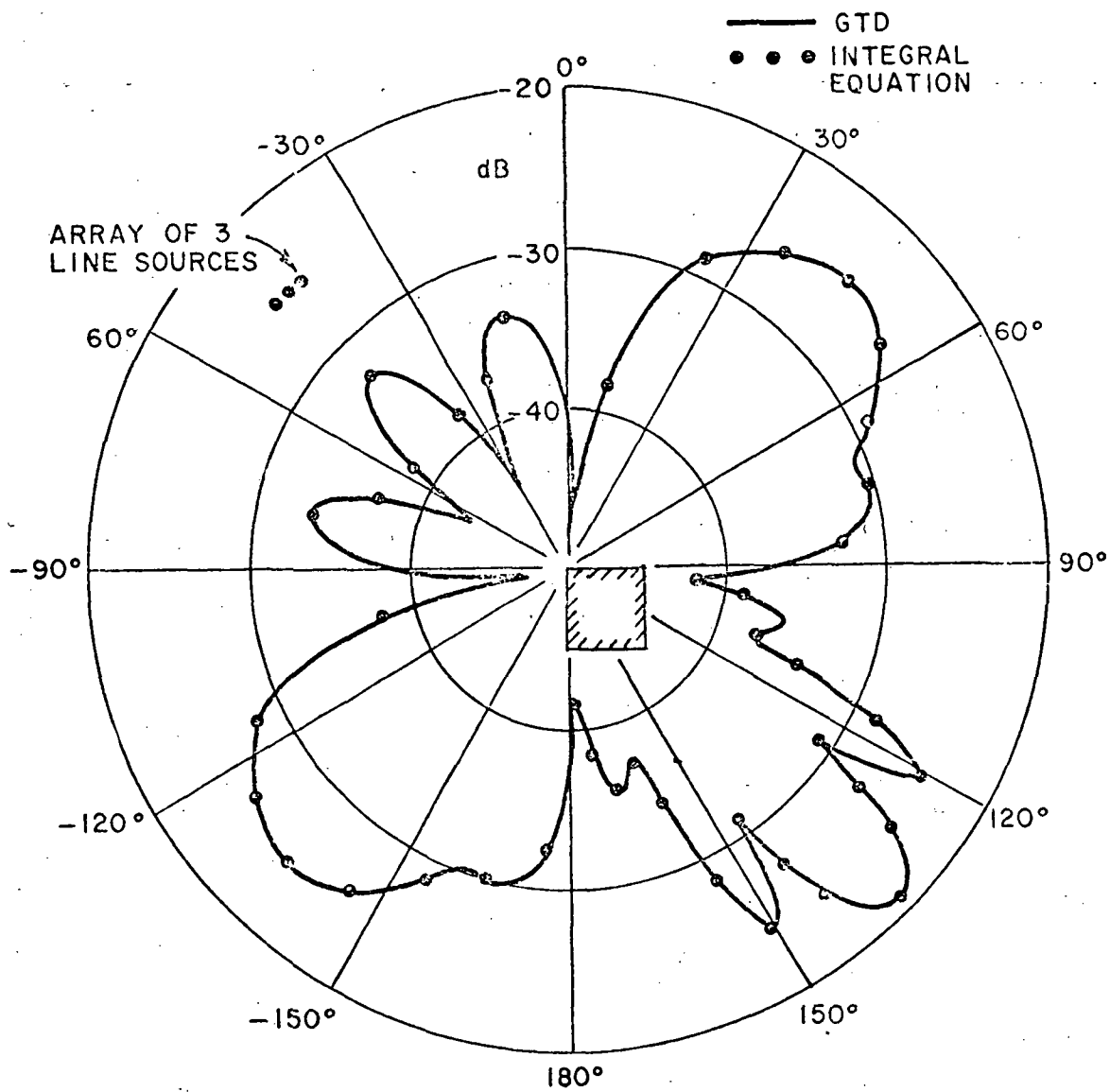


Fig. 20. Pattern of the field scattered by a square cylinder which is illuminated by an array of three magnetic line sources.

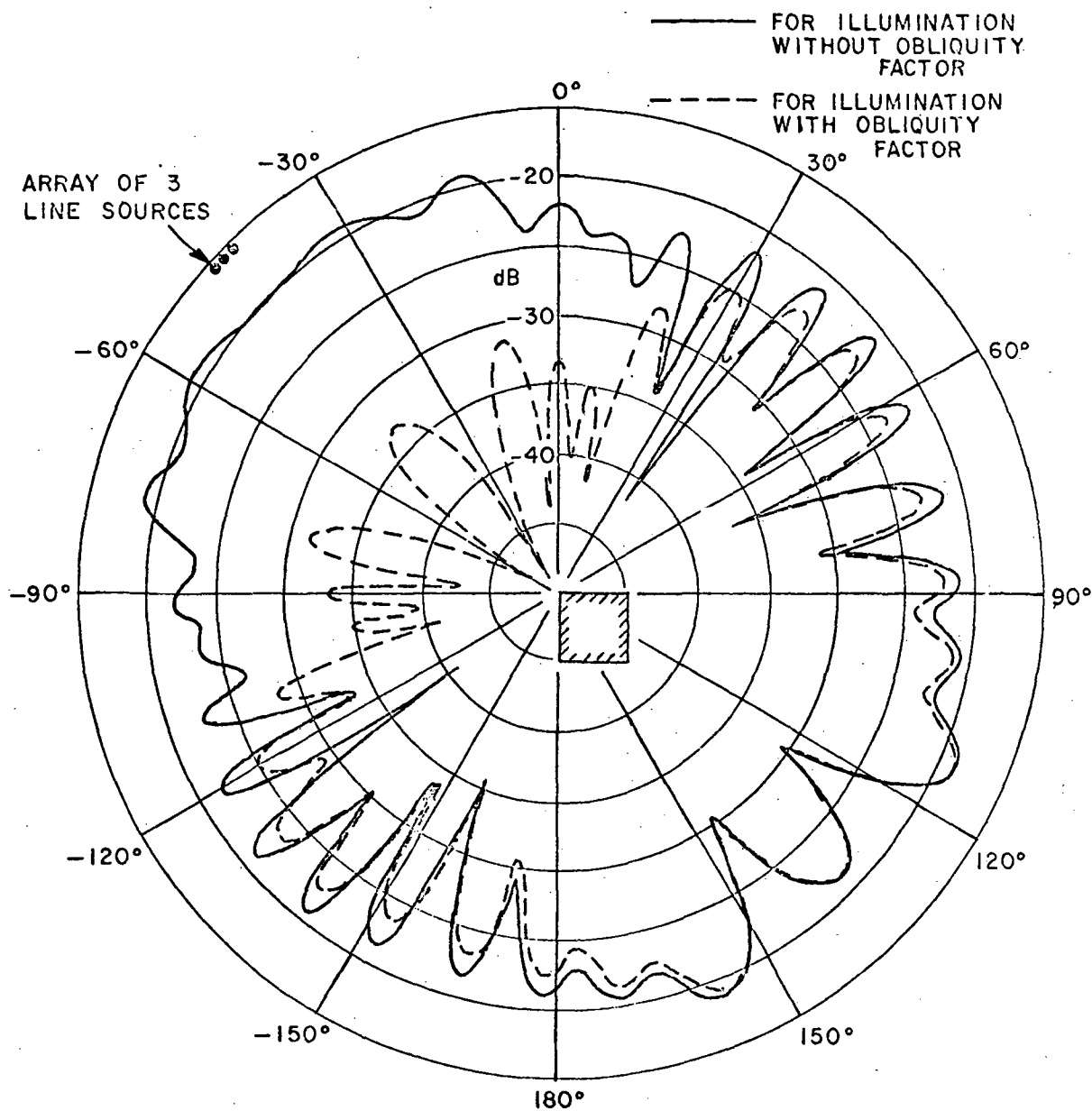


Fig. 21. Pattern of an array of three magnetic line sources in the presence of a square cylinder.

# G. Listing of the Computer Programs

```

PROGRAM LSOSBOX(INPUT,OUTPUT,TAPE5=INPUT,TAPE6=OUTPUT)
PROGRAM LSOSBOX IS PHENIX AUGUST 1972

C N THE NUMBER OF LINE SOURCES OR ELEMENTS IN THE ARRAY
C TYPE 1.0 IS ELECTRIC CURRENT LINE SOURCE
C TYPE 2.0 IS MAGNETIC CURRENT LINE SOURCE
C TYPE 3.0 IS MAGNETIC CURRENT MOMENT LINE SOURCE
C AL APERTURE WIDTH
C AM(1) MAGNITUDE OF THE(1)TH ELEMENT
C AP(1) PHASE OF THE(1)TH ELEMENT
C A(1) FIELD STRENGTH OF THE(1)TH ELEMENT
C U(1) SPACING BETWEEN(1+1)TH AND(1)TH ELEMENTS
C XLAMCA TRANSMITTED WAVELENGTH
C X THE POINT OF INCIDENCE
C XL THE LENGTH OF THE BOX
C H THE HEIGHT OF THE BOX
C RI INCIDENCE RANGE
C RS SCATTERING RANGE
C THI ANGLE OF INCIDENCE 0 TO 65
C THS ANGLE OF SCATTERING -65 TO 65
C XP,YP OBSERVING POINT
C XS(1),YS(1) SOURCE POINT OF THE(1)TH ELEMENT
C DS DIFFRACTION COEFFICIENT FOR SOFT BOUNDARY
C DH DIFFRACTION COEFFICIENT FOR HARD BOUNDARY
C GA(1) DIRECT INCIDENT FIELD DUE TO(1)TH ELEMENT
C RA(1) REFLECTED FIELD DUE TO(1)TH ELEMENT
C DAR1(1) FIRST ORDER DIFFRACTED FIELD FROM THE RIGHT EDGE DUE TO(1)TH ELEMENT
C DAR2(1) 2ND ORDER DIFFRACTED FIELD FROM THE RIGHT EDGE DUE TO(1)TH ELEMENT
C DAR3(1) 3RD ORDER DIFFRACTED FIELD FROM THE RIGHT EDGE DUE TO(1)TH ELEMENT
C DAL1(1) FIRST ORDER DIFFRACTED FIELD FROM THE LEFT EDGE DUE TO(1)TH ELEMENT
C DAL2(1) 2ND ORDER DIFFRACTED FIELD FROM THE LEFT EDGE DUE TO(1)TH ELEMENT
C DAL3(1) 3RD ORDER DIFFRACTED FIELD FROM THE LEFT EDGE DUE TO(1)TH ELEMENT
C TA(1) THE FIELD AT THE OBSERVING POINT DUE TO(1)TH ELEMENT
C TOTAL TOTAL FIELD AT OBSERVING POINT DUE TO ALL THE ELEMENTS
C DBAL MAGNITUDE OF THE TOTAL FIELD EXPRESSED IN DB
C DBSAS MAGNITUDE OF THE SCATTERED FIELD EXPRESSED IN DB
C DBHA DIRECT INCIDENT FIELD EXPRESSED IN DB
C PHASE PHASE OF THE TOTAL FIELD EXPRESSED IN DEGREES
C ATAL AMPLITUDE OF TOTAL FIELD AND ALSO OF INCIDENT FIELD IN SUBROUTINE TEST

C DIMENSION DAL(100)
C DIMENSION CAL(51),DAL2(51),DAL3(51),TA(51)

```

000003  
000003



```

000221      CALL PSFJDV
000222      READ(5,1110) N, TYPE,AL,SOURCE
000236      1110 FORMAT(110,2F10.4,A8)
000236      WRITE(6,2110)N,TYPE,AL,SOURCE
000252      2110 FORMAT(/,3X12*ELEMENTS*3X*TYPE= *F3.1,3X*APERTURE WIDTH=*F7.4,3X
          1A8* CURRENT LINE SOURCE*/)
000252      READ(5,1114) ( AM(I),AP(I) , I=1,N )
000267      1114 FORMAT( 1CF8.4 )
000267      PRINT 2114, (I,AM(I),AP(I) , I=1,N )
000305      2114 FORMAT (/15X*AM*10X*AP*/(5X*N(I2*))*2F10.4))
000305      PRINT 8889
000311      8889 FORMAT (1H1)
000311      ANN=N-1
000313      IF (N.EQ.1) GO TO 6666
000314      DO 1000 JJ=1,N
000316      D(JJ)=AL/FLOAT(NNN)
000321      1000 CONTINUE
000323      GU TO 7777
000323      6666 D(1)=0.0
000324      7777 CONTINUE
000324      DO 1115 M=1,N
000326      A(M)=AM(M)*CEXP( CMPLX(0.0,AP(M) ) )
000343      WRITE(6,665) M,A(M)
000354      665 FORMAT(5X,*A(*12,*))*2F10.4)
000354      1115 CONTINUE
000357      6789 CONTINUE
000401      READ(5,1111) XLAMDA,X,XL,H,RI,RS,THI
000401      1111 FORMAT(7F10.4 )
000401      IF (EUF,5)1112,6790
000404      6790 CONTINUE
000404      WRITE(6,2111) XLAMDA,X,XL,H,RI,RS,THI
000426      2111 FORMAT(1H1,5X,*LAMDA= *F7.4,* X= *F7.4,* L= *F7.4,* H= *,
          1F7.4,* RI= *,F7.4,* RS= *,F9.4,* THI= *,F7.4///// )
C
000426      PI=3.1415926535898
000427      TP=2.*PI
000431      STP=SQRT(TP)
000433      SQRTPI=SQRT(PI)
000435      TT=PI/180.
000437      TTDEG=180./PI

```

```

000440      PIU2=0.5*PI
000442      PIU4=.25*PI
000444      XLNCRM=1.0/XLAMDA
000445      R=1.0
*
000446      IF (TYPE.NF.2.C) R=-1.0
000452      XLW=XL/XLAMCA
000453      HW=H/XLAMDA
000455      THI=THI*TT
*
000457      L=181
C      L IS 1-GT.THE NUMBER OF POINTS,NPTS, TO BE PLOTED
C
000460      THS=181.0
000462      GO TO 5598
*
000464      9999 CONTINUE
000466      THS=THS*TTDEG
000468      ATAL=0.
000469      CBTAL=0.
000471      DBGA=0.
000473      CBSAS=0.
000475      PHASE=0.
000477      PRINT 4, THS,ATAL,CBTAL,DBGA,CBSAS,PHASE
000510      IF ( ATAL.EQ.0.0) GO TO 5
*
000511      9998 CONTINUE
000513      I=1
000515      THS=THS-2.0
000517      IF (THS.LT.-180.0) GO TO 1
000519      THS=THS*TT
000521      XS(I)=X-RI*SIN(THI)
000523      YS(I)=Y+RI*COS(THI)
000525      XP=X+RS*SIN(THS)
000527      YP=Y+RS*COS(THS)
000529      TE=ATAN2(YP,XP)
000531      TB=ATAN2(YP,XP-XL)
000533      20 CONTINUE
000535      TC=ATAN2(YS(I),XL-XS(I))
000537      TD=ATAN2(YS(I),-XS(I))
*
000564      BOND=0.01*TT
*
12900000
13000000
13100000
13200000
13300000
13400000
13500000
13600000
13700000
13800000
13900000
14000000
14100000
14200000
14300000
14400000
14500000
14600000
14700000
14800000
14900000
15000000
15100000
15200000
15300000
15400000
15500000
15600000
15700000
15800000
15900000
16000000
16100000
16200000
16300000
16400000
16500000
16600000
16700000
16800000
16900000
17000000
17100000

```

000573  
000577  
000603

IF( ABS(TH-PIQ2 ).LE.BOND ) GO TO 9999  
IF( ABS(TH-PIQ2 ).LE.BOND ) GO TO 9999  
IF( ABS(TH-TC).LE.BOND ) GO TO 9999  
IF( ABS(TE-TD).LE.BOND ) GO TO 9999

\*  
C  
C  
C

ANY ONE OF THE 11 IF STATEMENTS ENDING IN GO TO 9999 MAY CAUSE THE  
CURRENT ODD NUMBERED THIS ANGLE IN DEG TO BE SKIPPED

000607  
000616  
000633  
000634  
000647  
000660  
000667  
000701  
000710  
000721  
000732  
000740  
000747  
000754  
000765  
000774  
001003  
001014  
001016  
001022  
001030  
001041  
001043

XR=(XP\*YS(I)+XS(I)\*YP)/((YS(I)+YP )  
RO(I)=SQRT((XP-XS(I))\*((XP-XS(I))\*((XP-YS(I))\*((YP-YS(I)))/XLAMDA  
OE(I)=PI  
IF(ABS(THS+THI).GT.BCND) OB(I)=FA(RS,RI,RO(1)\*XLAMDA)  
R1=WLNRM \*SQRT( (XR-XS(I))\*((XR-XS(I))\*((-YS(I))\*((-YS(I)) )  
R2=WLNRM \*SQRT( (XP-XH)\*((XP-XR))\*((YP\*YP) )  
R3=WLNRM \*SQRT( (XL-XS(I))\*((XL-XS(I))\*((-YS(I))\*((-YS(I)) )  
R4=WLNRM \*SQRT( (XP-XL)\*((XP-XL))\*((YP\*YP) )  
R5=WLNRM \*SQRT( (XP-XL)\*((XP-XL))\*((YP+H )\*(YP+H ) )  
R6=WLNRM \*SQRT( (-XS(I))\*((-XS(I))\*((-YS(I))\*((-YS(I)) )  
R7=WLNRM \*SQRT( (XP\*XP)+((YP\*YP) )  
R8=WLNRM \*SQRT( (XP\*XP)+((YP+H )\*(YP+H ) )  
THK=ATAN2(YP,XP-XR)  
R9=WLNRM \*SQRT(XS(I)\*XS(I)+((YS(I)+H)\*((YS(I)+H) )  
PHI=(PI-ATAN2(YS(I),XS(I)-XL) ) \*TTDEG  
PH1=(PI-ATAN2(YP,XP-XL) ) \*TTDEG  
PH2=(PI-ATAN2(XP-XL,-H-YP) ) \*TTDEG  
PH3=270.0-PHI  
THP=(ATAN2(YS(I),XS(I)) ) \*TTDEG  
TH1=(PI-ATAN2(YP,-XP) ) \*TTDEG  
TH2=(PI-ATAN2(-XP,-H-YP) ) \*TTDEG  
TH3=270.0-TH1  
TH4=ATAN2((-XS(I),YS(I)+H)

C

IF(XS(I).LT.0.0.AND.ABS((TH1-THS)/TT-180.0).LE.1.0) GO TO 9999  
IF(XS(I).GE.0.0.AND.ABS((TH1-THP-180.0).EQ.0.0) GO TO 9999  
IF(XS(I).LT.0.0.AND.ABS((TH2-TH4/TT-180.0).EQ.0.0) GO TO 9999  
IF(ABS(PHI-PHP-180.0).EQ.0.0) GO TO 9999

C

QA=G(R3,R4 )  
CALL DFRCE( DA,1.5,CA,PH1-PHP,1.0)  
CALL DFRCE( DR,1.5,QA,PH1+PHP,1.0)  
DK1 =DH(DA,DB)

\*\*  
\*\*

001116  
001121  
001126  
001134

17200000  
17300000  
17400000  
17500000  
17500000  
17700000  
17800000  
17900000  
18000000  
18100000  
18200000  
18300000  
18400000  
18500000  
18500000  
18700000  
18900000  
18900000  
19000000  
19100000  
19200000  
19300000  
19400000  
19500000  
19500000  
19700000  
19800000  
19900000  
20000000  
20100000  
20200000  
20300000  
20400000  
20500000  
20600000  
20700000  
20800000  
20900000  
21000000  
21100000  
21200000  
21300000  
21400000



21500000  
21500000  
21700000  
21300000  
21900000  
22000000  
22100000  
22200000  
22300000  
22400000  
22500000  
22600000  
22700000  
22800000  
22900000  
23000000  
23100000  
23200000  
23300000  
23400000  
23500000  
23600000  
23700000  
23800000  
23900000  
24000000  
24100000  
24200000  
24300000  
24400000  
24500000  
24600000  
24700000  
24800000  
24900000  
25000000  
25100000  
25200000  
25300000  
25400000  
25500000  
25600000  
25700000

```
IF (TYPE,NE,2,0) . DRL=DS(DA,DB)
QB=G(R3,HW)
CALL DFRCF(DC,1.5,QB,270.00-THP,1.0)
CALL DFRCF(DD,1.5,QB,270.00+THP,1.0)
DR21=DH(DC,DD)
IF (TYPE,NE,2,0) DR21=DS(DC,DD)
QC=G(HW,R5)
CALL DFRCF(DE,1.5,QC,PH2+0.0,1.0)
CALL DFRCF(DF,1.5,QC,PH2-0.0,1.0)
DR22=DH(DE,DF)
IF (TYPE,NE,2,0) DR22=DS(DE,DF)
DR31=DR21
CALL DFRCF(DG,1.5,HW,C,0,1.0)
CALL DFRCF(DZ,1.5,HW,0,0,1.0)
DR32=DH(DG,DZ)
IF (TYPE,NE,2,0) DR32=DS(DG,DZ)
QD=G(HW,R4)
CALL DFRCF(DI,1.5,QD,PH3,1.0)
CALL DFRCF(DJ,1.5,QD,PH3,1.0)
DR33=DH(DI,DJ)
IF (TYPE,NE,2,0) DR33=DS(DI,DJ)
QE=G(R6,R7)
CALL DFRCF(DK,1.5,QE,TH1-THP,1.0)
CALL DFRCF(DL,1.5,QE,TH1+THP,1.0)
DL1=EF(DK,DL)
IF (TYPE,NE,2,0) DL1=DS(DK,DL)
QF=G(R6,HW)
CALL DFRCF(DM,1.5,QF,270.00-THP,1.0)
CALL DFRCF(DN,1.5,QF,270.00+THP,1.0)
DL21=DH(DM,DN)
IF (TYPE,NE,2,0) DL21=DS(DM,DN)
QG=G(HW,R8)
CALL DFRCF(DO,1.5,QG,TH2,1.0)
CALL DFRCF(DP,1.5,QG,TH2,1.0)
DL22=DH(DO,DP)
IF (TYPE,NE,2,0) DL22=DS(DO,DP)
DL31=DL21
CALL DFRCF(DQ,1.5,HW,0,0,1.0)
CALL DFRCF(DR,1.5,HW,0,0,1.0)
DL32=DH(DQ,DR)
IF (TYPE,NE,2,0) DL32=DS(DQ,DR)
QI=G(HW,R7)
CALL DFRCF(DX,1.5,QI,TH3,1.0)
```

001143  
001154  
001157  
001154  
001172  
001201  
001212  
001215  
001222  
001230  
001237  
001250  
001253  
001256  
001262  
001271  
001302  
001305  
001310  
001314  
001323  
001334  
001337  
001344  
001352  
001361  
001372  
001375  
001402  
001410  
001417  
001430  
001433  
001436  
001442  
001451  
001462  
001465  
001470  
001474  
001503  
001514  
001517

001225	CALL DFRCF(DY,1.5,Q1,TH3,1.0)	25900000
001535	DL33=LF(DX,DY)	25900000
001546	IF(TYPE.NE.2.0) DL33=DS(DX,DY)	26000000
001551	GK=G(R8,K9)	26100000
001557	CALL DFRCF(ZA,1.5,QK,TH2-TH4/TT,1.0)	26200000
001566	CALL DFRCF(ZB,1.5,QK,TH2+TH4/TT,1.0)	26300000
001575	DLL=OH(ZA,ZB)	26400000
001606	IF(TYPE.NE.2.0) DLL=DS(ZA,ZB)	26500000
001632	DAL(1)=A(1)*F(R9)*DLL*(R8)	26600000
001642	GAL(1)=DAL(1)*F(TH1-TH4)	26700000
001655	GA(1)=A(1)*F(R0(1))	26800000
001655	GA(1)=GA(1)*F(OB(1))	26900000
001701	RA(1)=A(1)*R*(R1+R2)	27000000
001717	RA(1)=RA(1)*F(TH1-ATAN2(VS(1),ABS(XR-XS(1))))	27100000
001743	DAR1(1)=A(1)*F(R3)*DR1*(R4)	27200000
001756	DAR1(1)=DAR1(1)*F(0.5*PI-TH1-PHP*TT)	27300000
002014	DAR2(1)=A(1)*F(R3)*DR21*(HW)*0.5*DR22*(R5)	27400000
002027	DAR2(1)=DAR2(1)*F(0.5*PI-TH1-PHP*TT)	27500000
002053	DAL1(1)=A(1)*F(R6)*DL1*(R7)	27600000
002066	DAL1(1)=DAL1(1)*F(0.5*PI+TH1-THP*TT)	27700000
002124	DAL2(1)=A(1)*F(R6)*DL21*(HW)*0.5*DL22*(R8)	27900000
002137	DAL2(1)=DAL2(1)*F(0.5*PI+TH1-THP*TT)	27900000
002147	IF(XS(1).EQ.0.0) DAL2(1)=0.5*DAL(1)	28000000
002153	YL2=G(R8,R6+H)	28100000
002161	XF=2.0*(R6,H+R8)	28200000
002167	CALL CS(C,S,XF)	28300000
002173	CALL WANG(TH2,0.0,1.5,YL2,HA,HB)	28400000
002243	CALL WANG(270.0,0.0,1.5,YL2,HC,HD)	28500000
002247	PLUS=A(1)*F(R6)*FL(XF,C,S)*COT(TP/3.0)*PW(0.125)*F(-HW)/3.0/SIP	28600000
002270	IF(TYPE.NE.2.0) HA=HB	28700000
002306	IF(XS(1).EQ.0.0) DAL2(1)=DAL2(1)+PLUS*(R8)	28800000
002316	IF(XS(1).EQ.0.0) DAL2(1)=DAL2(1)+PLUS*(R8)	28900000
002325	IF(XS(1).FQ.0.0) AND(TYPE.EQ.1.0) DAL2(1)=CMPLX(0.0,0.0)	29000000
002333	IF(XS(1).GE.0.0) DAL(1)=CMPLX(0.0,0.0)	29100000
002335	DAL3(1)=CMPLX(0.0,0.0)	29200000
002343	DAR3(1)=CMPLX(0.0,0.0)	29300000
002352	WX=G(R9,HW)	29400000
002361	CALL DFRCF(ZX,1.5,WX,0.0-TH4/TT,1.0)	29500000
	CALL DFRCF(ZY,1.5,WX,0.0+TH4/TT,1.0)	29600000
	DLB=OH(ZX,ZY)	29700000
	IF(TYPE.NE.2.0) DLB=DS(ZX,ZY)	29800000
		29900000
		30000000

```

002372      DALB(I)=A(I)*F(R9)*ELB*0.5*F(HW)*DL33*F(R7)
002430      DALB(I)=DALB(I)*F8(THI-TH4)
002440      IF(XS(I).GT.0.0) DALB(I)=CMPLX(0.0,0.0)
002450      IF(THI.GT.270.0.AND.0.0) DALB(I)=CMPLX(0.0,0.0)

C
002467      RLO=SQRT((XP-XL)*(XP-XL)+(YP+H)*(YP+H))/XL4*DA
002500      TH5=(PI-ATAN2(-YP,XP-XL))*TTDEG
002510      PA=G(R9,XLW)
002513      CALL DFRCF(ZP,1.5,PA,270.0-TH4/TT,1.0)
002521      CALL DFRCF(ZC,1.5,PA,270.0+TH4/TT,1.0)
002530      DBL1=DH(ZP,ZQ)
002537      IF(TYPE.NE.2.0) DBL1=DS(ZP,ZQ)
002550      PB=G(XLW,R10)
002553      CALL DFRCF(ZR,1.5,PB,0.0-TH5,1.0)
002560      CALL DFRCF(ZS,1.5,PB,0.0+TH5,1.0)
002566      DBL2=DH(ZR,ZS)
002575      IF(TYPE.NE.2.0) DBL2=DS(ZR,ZS)
002606      DB2(I)=A(I)*F(R9)*CBL1*F(XLW)*0.5*DBL2*F(R10)
002644      DB2(I)=DB2(I)*F8(THI-TH4)
002654      IF(XS(I).GT.0.0) DB2(I)=CMPLX(0.0,0.0)
002664      IF(XS(I).EQ.0.0) DB2(I)=0.5*DB2(I)
002674      IF(TYPE.NE.2.0) HC=H
002701      IF(XS(I).EQ.0.0) DB2(I)=DB2(I)-PLUS*HC*F(XLW)*DBL2*F(R10)
002733      IF(TH5.GT.270.0.AND.0.0) DB2(I)=CMPLX(0.0,0.0)
002752      QX=G(R3,XLW)
002755      CALL DFRCF(ZG,1.5,QX,0.0-PHP,1.0)
002762      CALL DFRCF(ZH,1.5,QX,0.0+PHP,1.0)
002770      DLR1=DF(ZG,ZH)
002777      IF(TYPE.NE.2.0) DLR1=DS(ZG,ZH)
003010      LW=G(R7,XLW)
003013      CALL DFRCF(ZM,1.5,LW,THI,1.0)
003016      CALL DFRCF(ZN,1.5,LW,THI,1.0)
003022      DLR2=DH(ZM,ZN)
003031      IF(TYPE.NE.2.0) DLR2=DS(ZM,ZN)
003042      DLR(I)=A(I)*F(R3)*DLR1*F(XLW)*0.5*DLR2*F(R7)
003100      DLR(I)=DLR(I)*F8(0.5*PI-THI-PHP*TT)
003113      IF(THI.GT.270.0.AND.0.0) DLR(I)=CMPLX(0.0,0.0)
003131      QZ=G(R6,XLW)
003134      CALL DFRCF(ZC,1.5,QZ,0.0-THP,1.0)
003141      CALL DFRCF(ZD,1.5,QZ,0.0+THP,1.0)
003147      DRL1=DH(ZC,ZD)
003156      IF(TYPE.NE.2.0) DRL1=DS(ZC,ZD)
003157      QY=G(XLW,R4)

```

003172  
003175  
003201  
003210

CALL DFKCF(ZF,1.5,QY,PH1,1.0)  
CALL DFKCF(ZF,1.5,CY,PH1,1.0)  
DRL2=DH(ZF,ZF)  
IF(TYPE,NE.2.0) DRL2=DS(ZE,ZF)

\*\*  
\*\*

003221  
003257  
003272  
003310  
003317

DRL(I)=A(I)\*F(R6)\*DRL1\*(XLW)\*0.5\*DRL2\*(R4)  
DRL(I)=DRL(I)\*FB(0.5\*PI+THI-THP\*TT)  
IF(PH1-GE.270.0.AND.PH1.LT.360.) DRL(I)=CMPLX(0.0,0.0)  
ADDSA(I)=CMPLX(0.0,C.0)  
CALL KKDC(CX,1.5,QK,0.0,TH2,1.0,1)

\*  
\*

003325  
003406  
003415  
003423  
003434

IF(TYPE,EQ.1.0.AND.TH2.GT.0.0.AND.TH2.LT.270.0.AND.XS(I)-EQ.0.0)  
1ADUSA(I)=A(I)\*F(R9)\*0.5\*SQRT(IP)\*CX\*(R8)/CMPLX(0.0,R9\*TP)\*2.0  
ADDSB(I)=CMPLX(0.0,C.0)  
CALL KKDC(CY,1.5,QB,PHP,270.0,1.0,0)  
CALL KKDC(CZ,1.5,QC,0.0,270.0-TH5,1.0,1)  
IF(TYPE,EQ.1.0.AND.TH5.GT.0.0.AND.TH5.LT.270.0)  
1ADDSB(I)=A(I)\*F(R3)\*F(HW)\*CY\*TP\*0.5\*CZ\*(R10)/CMPLX(0.0,HW\*TP)  
ADUSC(I)=CMPLX(0.0,0.0)  
CALL KKDC(CV,1.5,QF,90.0,270.0,1.0,0)  
CALL KKDC(CW,1.5,QG,0.0,TH2,1.0,1)

003515  
003524  
003532  
003541  
003626  
003633  
003642  
003650  
003657

IF(TYPE,EQ.1.0.AND.TH2.GT.0.0.AND.TH2.LT.270.0.AND.XS(I)-EQ.0.0)  
1ADUSC(I)=A(I)\*F(R6)\*CX\*(HW)\*0.5\*CW\*(R8)/CMPLX(0.0,TP\*HW)  
ADUSC(I)=ADUSC(I)\*IP  
ADUSD(I)=CMPLX(0.0,0.0)  
CALL KKDC(CVV,1.5,QX,PHP,0.0,1.0,0)  
CALL KKDC(CWW,1.5,CW,0.0,TH1,1.0,1)  
IF(TYPE,EQ.1.0.AND.TH1.GT.0.0.AND.TH1.LT.270.0)  
1ADUSD(I)=A(I)\*F(R3)\*CVV\*(XLW)\*0.5\*CW\*(R7)/CMPLX(0.0,XLW\*TP)  
ACUSC(I)=ACUSD(I)\*TP

\*  
\*

003737  
003744  
003765  
004011  
004015  
004037  
004053  
004072  
004111

ACUSC(I)=ACUSD(I)\*TP  
IF(TYPE,EQ.3.0.AND.OB(I).LT.PI/2.0) GA(I)=GA(I)\*COS(OB(I))  
IF(TYPE,EQ.3.0.AND.CB(I).GT.PI/2.0) GA(I)=GA(I)\*COS(PI-OB(I))  
GGA(I)=GA(I)  
IF(TYPE,EQ.3.0) RA(I)=KA(I)\*COS(THI-ATAN2(YS(I),ABS(XR-XS(I))))  
IF(TYPE,EQ.3.0) DAL(I)=DAL(I)\*COS(THI-TH4)  
IF(TYPE,EQ.3.0) DAR1(I)=DAR1(I)\*COS(0.5\*PI-THI-PHP\*TT)  
IF(TYPE,EQ.3.0) DAR2(I)=DAR2(I)\*COS(0.5\*PI-THI-PHP\*TT)  
IF(TYPE,EQ.3.0) DALL(I)=DALL(I)\*CCS(0.5\*PI+THI-THP\*TT)

34400000  
34500000  
34600000  
34700000  
34800000  
34900000  
35000000  
35100000  
35200000  
35300000  
35400000  
35500000  
35600000  
35700000  
35800000  
35900000  
36000000  
36100000  
36200000  
36300000  
36400000  
36500000  
36600000  
36700000  
36800000  
36900000  
37000000  
37100000  
37200000  
37300000  
37400000  
37500000  
37600000  
37700000  
37800000  
37900000  
38000000  
38100000  
38200000  
38300000  
38400000  
38500000  
38600000

```

004130      IF (TYPE.EQ.3.0) DAL2(I)=DAL2(I)*COS(0.5*PI+THI-THP*TT)
004147      IF (TYPE.EQ.3.0) DALB(I)=DALB(I)*COS(THI-TH4)
004163      IF (TYPE.EQ.3.0) DB2(I)=DB2(I)*COS(THI-TH4)
004177      IF (TYPE.EQ.3.0) DLR(I)=DLR(I)*COS(0.5*PI-THI-THP*TT)
004216      IF (TYPE.EQ.3.0) DRL(I)=DRL(I)*COS(0.5*PI+THI-THP*TT)
      ***
004235      IF (YP.GT.0.0) GO TO 3333
004240      RA(I)=CMPLX(0.0,0.0)
004246      IF (XS(I).GE.0.0.AND.PHI-THP.EQ.180.0.OR .PHI-THP.EQ.180.)
      1 GO TO 9999
004264      IF (XS(I).GT.0.0.AND.PHI-THP.GE.180.0.AND.THI-THP.GE.180.0)GA(I)=
      1 CMPLX(0.0,0.0)
004312      IF (XS(I).LT.0.0.AND.PHI-THP.EQ.180.0.OR .(TH2-TH4/TT).EQ.180.0)
      1 GO TO 9999
004331      IF (XS(I).LT.0.0.AND.PHI-THP.GT.180.0.AND.(TH2-TH4/TT).GT.180.0)
      1 GA(I)=CMPLX(0.0,0.0)
004356      IF (PHI.LT.270.0.AND.PHI.LT.360.0) CAR1(I)=CMPLX(0.0,0.0)
004375      IF (TH1.GT.270.0.AND.THI.LT.360.0) DAL1(I)=CMPLX(0.0,0.0)
004414      IF (PH2.GE.270.0.AND.PH2.LT.360.0) CAR2(I)=CMPLX(0.0,0.0)
004433      IF (TH2.GE.270.0.AND.TH2.LT.360.0) CAL2(I)=CMPLX(0.0,0.0)
004452      IF (TH3.LF.0.0) DAL3(I)=CMPLX(0.0,0.0)
004463      IF (PH3.LF.0.0) CAR3(I)=CMPLX(0.0,0.0)
004474      IF (TH2.GF.270.0.AND.TH2.LJ.360.0) DAL(I)=CMPLX(0.0,0.0)
004513      IF (XS(I).LT.0.0.AND.XP.LT.0.0) RA(I)=A(I)*F(SQRT((XS(I)+XP)*
      1 (XS(I)+XP)+(YS(I)-YP)*(YS(I)-YP))/XLAMDA)
      YK=YP-XP*(YP-YS(I))/(XP+XS(I))
004550
004557      IF (YP.EQ.-H.(CR.YR.FC.0.0) GO TO 9999
      *
004566      IF (XS(I).LT.0.0.AND.XP.LT.0.0)
      1 RA(I)=RA(I)*F(ATAN2(-XS(I),YS(I)-YR)-THI)
      IF (XS(I).LT.0.0.AND.XP.LT.0.0.AND.TYPE.EQ.3.0)
      1 RA(I)=RA(I)*COS(THI-ATAN2(-XS(I),YS(I)-YR))
      IF (YK.LE.-H.(CR.YR.FC.0.0) RA(I)=CMPLX(0.0,0.0)
      TA(I)=GA(I)+RA(I)+CAR1(I)+CAR2(I)+DAR2(I)+DAR3(I)+DAL1(I)+DAL2(I)+DAL3(I)
      1 +DAL(I)
004723      TA(I)=TA(I)+DLR(I)+DRL(I)
004734      TA(I)=TA(I)+DB2(I)
004742      TA(I)=TA(I)+DALB(I)

```

```

38700000
38800000
38900000
39000000
39100000
39200000
39300000
39400000
39500000
39600000
39700000
39800000
39900000
40000000
40100000
40200000
40300000
40400000
40500000
40600000
40700000
40800000
40900000
41000000
41100000
41200000
41300000
41400000
41500000
41600000
41700000
41800000
41900000
42000000
42100000
42200000
42300000
42400000
42500000
42600000
42700000
42800000
42900000

```

```

005007 300(I)=TA(I)-GA(I)
004757 TA(I)=TA(I)+ACOSA(I)
004765 TA(I)=TA(I)+ADDSH(I)
004773 TA(I)=TA(I)+ADDSH(I)
005001 TA(I)=TA(I)+ADDSH(I)
005007 GO TO 4444
3333 CONTINUE
TA(I)=GA(I)+RA(I)+DAR1(I)+DAR2(I)+DAR3(I)+DAL1(I)+DAL2(I)+DAL3(I)
TA(I)=TA(I)+DLR(I)+ERL(I)
TA(I)=TA(I)+D82(I)
TA(I)=TA(I)+DALB(I)
TA(I)=TA(I)+ADDSH(I)
TA(I)=TA(I)+ACDSH(I)
TA(I)=TA(I)+ADDSH(I)
TA(I)=TA(I)+ADDSH(I)
IF(XP.GT.XL.AND.TB.LT.TC) TA(I)=TA(I)-RA(I)-DAL2(I)
IF(XS(I).GT.O.O.AND.XP.GT.XL.AND.TB.GT.TC) TA(I)=TA(I)-DAL2(I)
IF(XS(I).GT.O.O.AND.XP.LT.XL.AND.XP.GT.O.O) TA(I)=TA(I)-DAL2(I)
1-DAL2(I)
IF(XS(I).GT.O.O.AND.XP.LT.O.O.AND.TE.LT.TD) TA(I)=TA(I)-DAR2(I)
IF(XS(I).GT.O.O.AND.XP.LT.O.O.AND.TE.GT.TD) TA(I)=TA(I)-DAR2(I)
1-RA(I)
IF(XS(I).EQ.O.O.AND.XP.GT.XL.AND.TB.GT.TC) TA(I)=TA(I)-DAL2(I)
IF(XS(I).EQ.O.O.AND.XP.LT.XL.AND.XP.GT.O.O) TA(I)=TA(I)-DAL2(I)
1-DAR2(I)
IF(XS(I).EQ.O.O.AND.XP.LT.O.O) TA(I)=TA(I)-RA(I)-DAR2(I)
IF(XS(I).LT.O.O.AND.XP.GT.XL.AND.TB.GT.TC.AND.TE.LT.TD) TA(I)=
TA(I)-DAL2(I)
IF(XS(I).LT.O.O.AND.XP.GT.XL.AND.TB.GT.TC.AND.TE.GT.TD) TA(I)=
TA(I)-RA(I)-DAL2(I)
IF(XS(I).LT.O.O.AND.XP.LT.XL.AND.XP.GT.O.O.AND.TE.LT.TD) TA(I)=
TA(I)-DAL2(I)-DAR2(I)
IF(XS(I).LT.O.O.AND.XP.LT.XL.AND.XP.GT.O.O.AND.TE.GT.TD) TA(I)=
TA(I)-RA(I)-DAL2(I)-DAR2(I)
IF(XS(I).LT.O.O.AND.XP.LT.O.O) TA(I)=TA(I)-RA(I)-DAR2(I)+DAL(I)
SAS(I)=TA(I)-GA(I)
4444 CONTINUE
NN=(N-1)/2
II=I-NN
IF(I.EQ.N) GO TO 11
XS(I+1)=XS(I)-FLOAT(I)*D(I)*COS(THI)
IF(I.GT.NN) XS(I+1)=XS(I)+FLOAT(I)*D(I)*COS(THI)
YS(I+1)=YS(I)-FLOAT(I)*D(I)*SIN(THI)
005211 43000000
005233 43100000
005260 43200000
005303 43300000
005330 43400000
005350 43500000
005402 43600000
005437 43700000
005471 43800000
005526 43900000
005551 44000000
005560 44100000
005562 44200000
005564 44300000
005566 44400000
005575 44500000
005606 44600000
005636 44700000
005666 44800000
005706 44900000
005736 45000000
005766 45100000
005796 45200000
005826 45300000
005856 45400000
005886 45500000
005916 45600000
005946 45700000
005976 45800000
006006 45900000
006036 46000000
006066 46100000
006096 46200000
006126 46300000
006156 46400000
006186 46500000
006216 46600000
006246 46700000
006276 46800000
006306 46900000
006336 47000000
006366 47100000
006396 47200000

```

```

005626      IF (I-1) .GT. 1) YS(I) = YS(I) + FLDA(I) * D(I) * SIN(THI)
005630      N = I + 1
005633      RO(M) = SQRT((XP-XS(M)) * (XP-XS(M)) + (YP-YS(M)) * (YP-YS(M))) / XLAMDA
005644      UB(M) = FA(U(I)) * FLGAT(I) + RO(I) * XLAMDA, RO(M) * XLAMDA + OB(I)
005655      IF (I-1) .GT. NN) OB(M) = OB(I) - FA(FLOAT(I-NN)) * D(I), RO(I) * XLAMDA,
005672      RO(M) * XLAMDA
005672      IF (OB(I) .GT. PIO2) OB(M) = OB(I) - FA(U(I)) * FLOAT(I), RO(I) * XLAMDA,
005707      RO(M) * XLAMDA
005734      IF (CH(I) .GT. PIO2) .AND. I .GT. NN)
005740      IOB(M) = OB(I) + FA(FLOAT(I-NN)) * D(I), RO(I) * XLAMDA, RO(M) * XLAMDA
005741      IF (I-1) .GT. NNN) GO TO 11
005741      I = I + 1
005741      GO TO 20
005741      11 CONTINUE
005741      SATAL = CMPLX(0.0, 0.0)
005744      RATAL = CMPLX(0.0, 0.0)
005746      TOTAL = CMPLX(0.0, 0.0)
005751      DO 3 K = 1, N
005752      KATAL = RATAL + GGA(K)
005750      SATAL = SATAL + SAS(K)
005766      3 TOTAL = TOTAL + TA(K)
005776      ATAL = CAHS(TOTAL)
006000      DBTAL = 20.0 * ALOG10(ATAL)
006003      GAM = CAHS(RATAL)
006005      DBGA = 20.0 * ALOG10(GAM)
006010      SASM = CABS(SATAL)
006012      DBSAS = 20.0 * ALOG10(SASM)
006015      WK = REAL(TOTAL)
006017      WI = AIMAG(TOTAL)
006020      PHASE = ATAN2(WI, WK)
006023      THS = THS * TTDEG
006025      PHASE = PHASE * TTDEG
006027      WRITE(6,4) THS, ATAL, DBTAL, DBGA, DBSAS, PHASE
006046      4 FORMAT(5X, *THS = *, F7.2, 5X, *ATAL = *, E12.4, 5X, *DBTAL = *, E12.4, 5X,
*DBGA = *, F12.4, 5X, *DBSAS = *, E12.4, 5X, *PHASE = *, E12.4)
*
C L-1 STORES THE COMPUTED POINTS IN REVERSE ORDER IN THE ARRAY, THAT IS,
C      THS FROM -179 TO +179 DEG FOR CARTESIAN PLOTTING
C
*
006046      5 L = L - 1
006050      THSTFD(L) = THS
006052      AMPIFD(L) = ATAL

```

```

006053      DBTFD(L)=DBTAL
006055      PHTFD(L)=PHASE
006056      GU TO 9958
*
006057      1 CONTINUE
C      FIN) MAX AMPTFD
      AMAX=AMPTFD(1)
      TMAX=THSTFD(1)
006052      DO 6956 J=2,180
006064      IF (AMPTFD(J).EQ.0.) AMPTFD(J)=(AMPTFD(J-1)+AMPTFD(J+1))/2.
006070      IF (AMPTFD(J).LE.AMAX) GU TO 6956
006073      AMAX=AMPTFD(J)
006074      TMAX=THSTFD(J)
006076      6956 CONTINUE
*
C      NORMALIZE AMPTFD
      DO 6957 J=1,180
006100      AMPTFD(J)=AMPTFD(J)/AMAX
006102
006104      6957 CONTINUE
006106      PRINT 5553,AMAX,TMAX
006115      5553 FORMAT(//,* MAX AMPTFD=*F9.5* FOR THSTFD=*F3* DEG*)
*
006115      PRINT 29,(THSTFD(J),AMPTFD(J),DBTFD(J),PHTFD(J), J=1,180)
006135      29 FORMAT(///2X*THS*5X*AMPTFDCR*7X*DBTFD*8X*PHASE*/(F5.3(4XF10.5)))
*
006135      THSTFD(181)=-180.
006136      THSTFD(192)=30.
006140      AMPTFD(181)=0.
006140      AMPTFD(182)=.1
006142      PHTFD(181)=-180.
006142      PHTFD(182)=30.
006144      CALL PLTTFCP(THSTFD,PHTFD,180)
006146      CALL PLTTFD(THSTFD,AMPTFD,180)
*
*
*
C      REORDER THSTFD VS DBTFD IN THE ARRAY, FROM 1 TO 359 DEG, FOR POLAR PLOT
*
      KK=90
006151      DO 1113 J=1,90
006152      KK=KK+1
006154      TEMP=THSTFD(KK)
006156      THSTFD(KK)=THSTFD(J)+360
006157

```

```

51600000
51700000
51800000
51900000
52000000
52100000
52200000
52300000
52400000
52500000
52500000
52700000
52800000
52900000
53000000
53100000
53200000
53300000
53400000
53500000
53600000
53700000
53800000
53900000
54000000
54100000
54200000
54300000
54400000
54500000
54600000
54700000
54800000
54900000
55000000
55100000
55200000
55300000
55400000
55500000
55600000
55700000
55800000

```



```

006162 THSTFD(J)=TEMP
006164 TEMP=CBTFD(KK)
006165 DBTFD(KK)=DBTFD(J)
006167 DBTFD(J)=TEMP
006170 1113 CONTINUE
      ** IN LSCSBOX
      *
006172 FIELD=5HTOTAL
006173 DMAX=DBTFD(1)
006174 TMAX=THSTFD(1)
006176 DO 6958 J=2,180
006200 IF (DBTFD(J).EQ.0.) DBTFD(J)=(DBTFD(J-1)+DBTFD(J+1))/2.
006204 IF (CBTFD(J).LE.DMAX) GO TO 6958
006207 DMAX=DBTFD(J)
006210 TMAX=THSTFD(J)
006212 6958 CONTINUE
      *
      C NORMALIZE DBTFD
006214 DO 6959 J=1,180
006216 DBTFD(J)=DBTFD(J)-DMAX
006220 IF (CBTFD(J).LT.-40.) CBTFD(J)=-40.
006224 6959 CONTINUE
006226 PRINT 5554,DMAX,TMAX
006236 5554 FORMAT(/// * MAX DBTFD=#F9.5# FOR THSTFD=#F3# DEC#)
006236 5555, (THSTFD(J),CBTFD(J),J=1,180)
006252 5555 FORMAT(/// * THSTFD*7X*DBTFDNOR*/(2XF3.8XF10.5))
      *
006252 CALL POLPLT(THSTFD,CBTFD,180,7.5,8,1,N,TYPE,AL,XLAMDA,X,XL,H,RI,RS
      1,TH1,DMAX,FIELD,SOURCE)
006275 PRINT 8888
006301 8888 FORMAT(///)
      *
006301 CALL TEST(N,AL,RS+RI,A,TYPE,SOURCE)
006307 GU TO 6789
006310 1112 CONTINUE
006310 CALL CALPLT(0.,0.,559)
006313 STOP
006315 END

```

```

C
C
C
C
C
*
000010 SUBROUTINE DFRCF(D,XA,Y,B,XLMCA)
000010 THIS ROUTINE IS TO COMPUTE THE DIFFRACTION COEFFICIENT
000010 COMPLEX F1J,F2J,Q,R,T1,D1,T2,D2,D,F1,F2,S
000010 COMMON/PICCNST/PI,TWOPI,STP,SQRTPI,TI,TTDEG,PI02,PI04
000010 BR=B*TI
000010 ARG1=(PI+BR)/(2.0*XN)
000010 ARG2=(PI-BR)/(2.0*XN)
000010 CX1=COS(ARG1)
000010 CX2=CCS(ARG2)
000010 SX1=SIN(ARG1)
000010 SX2=SIN(ARG2)
000010 X1=(BR+PI)/(2.0*XN*PI)
000010 N1=X1
000010 E1=X1-N1
000010 IF(E1.GT.0.5) N1=N1+1
000010 IF(E1.LT.-0.5) N1=N1-1
000010 FN1=FLOAT(N1)
000010 X2=(BR-PI)/(2.0*XN*PI)
000010 N2=X2
000010 E2=X2-N2
000010 IF(E2.GT.0.5) N2=N2+1
000010 IF(E2.LT.-0.5) N2=N2-1
000010 FN2=FLOAT(N2)
000010 A1=1.0+COS(-BR+2.0*XN*PI*FN1)
000010 A2=1.0+COS(-BR+2.0*XN*PI*FN2)
000010 SAI=SQRT(A1)
000010 SA2=SQRT(A2)
000010 XX=(SQRT(TWOPI*Y))*SA1
000010 YY=(SQRT(TWOPI*Y))*SA2
000010 XXS=XX*XX
000010 YYS=YY*YY
000010 PQ=SQRT(PI02)
000010 CALL CS(C1,S1,XXS)
000010 CCI=0.5-C1
000010 SSI=0.5-S1
000010 F1J=PC*CMPLX(SS1,CCI)
000010 CALL CS(C2,S2,YYS)
000010 CC2=0.5-C2
59700000
59800000
59900000
60000000
60100000
60200000
60300000
60400000
60500000
60600000
60700000
60800000
60900000
61000000
61100000
61200000
61300000
61400000
61500000
61600000
61700000
61800000
61900000
62000000
62100000
62200000
62300000
62400000
62500000
62600000
62700000
62800000
62900000
63000000
63100000
63200000
63300000
63400000
63500000
63600000
63700000
63800000

```

63900000  
64000000  
64100000  
64200000  
64300000  
64400000  
64500000  
64600000  
64700000  
64800000  
64900000  
65000000  
65100000

```

SS2=0.5-S2
F2J= PQ*CMPLX(SS2,CC2)
P=-PI04
Q=CMPLX(0.0,P)
R=CEXP(Q)
S=(1-0.25*R*SQRT(XLMDA))/(PI*XL)
T1=S*2.0*CEXP(CMPLX(0.0,XS))
U1=T1*F1J*CX1*(XX/SX1)
T2=S*2.0*CEXP(CMPLX(0.0,YS))
D2=T2*F2J*CX2*(YY/SX2)
D= D1+D2
RETURN
END

```

000207  
000211  
000221  
000222  
000225  
000227  
000234  
000270  
000302  
000316  
000330  
000340  
000341

65200000  
65300000  
65400000  
65500000  
65600000  
65700000  
65800000  
65900000  
66000000  
66100000  
66200000  
66300000  
66400000  
66500000  
66600000  
66700000  
66800000

```

SUBROUTINE KKDC(D,XN,XL,PHIP,PHI,XLMDA,T)
C - KARP - KELLER DIFFRACTION COEFFICIENT
XL - DISTANCE PARAMETER IN ANY UNIT
XLMDA - WAVELENGTH IN THE SAME UNIT
PHIP - ANGLE OF INCIDENCE IN DEGREES
PHI - ANGLE OF OBSERVATION IN DEGREES
XN - WEDGE ANGLE = (2.-XN)*PI
T - D/D(PHIP) OR D/D(PHI) = 1 OR 0
INTEGER T
COMPLEX D,D1,D2
BETAP=PHI+PHIP
BETAM=PHI-PHIP
CALL CC(D1,XN,XL,BETAP,XLMDA,1,T)
CALL CD(D2,XN,XL,BETAM,XLMDA,-1,T)
D=D2-D1
RETURN
END

```

C  
C  
C  
C  
C  
C  
C

000012  
000012  
000012  
000013  
000015  
000022  
000033  
000043  
000044

```

C
C
000012 SUBRCUTINE CD(D,XN,XL,BEIA,XLMCA,T1,T2)
000012 T1 - BETP OR BETM 1 OR -1
000012 T2 - C/D(PHIS) OR C/D(PHIO) 1 OR 0
C
000012 INTEGER T1,T2
000012 COMPLEX D,CP,CM,DP,DM,V,P,CCP,CCM,C,F1,F2
000012 P(X)=CEXP(CMPLX(.0,X))
C
000030 COMMON/PICONST/PI,TWCPI,STP,SCRIPTI,IT,ITDEG,PI02,PI04
*
000030 XK=TWOPI/XLMCA
000031 C=P(-PI04)/(4.*(XN**2)*SQRT(TWOPI*XK))
000053 BR=BETA*TT
000054 TP=(PI+BR)/(2.*XN)
000060 ATP=ABS(TP)
000062 IF(ATP.LT. 0.01)GO TO 10
000065 XNP=(BR+PI)/(2.*XN*PI)
000070 NP=XNP
000072 E1=XNP-NP
000074 IF(E1.GT. 0.5)NP=NP+1
000100 IF(E1.LT. -0.5)NP=NP-1
000104 AP=1.+COS(-BR+2.*XN*NP*PI)
000120 XKAP=XK*XL*AP
000122 CP=CEXP(CMPLX(.0,-PI04))/(4.*(XN**2)*SQRT(TWCPI*XK)*(SIN(PI+BR)/
1(2.*XN))**2))
CCP=CP*V(XKAP)
GO TO 11
10
000155 A1=2.*XK*XL*(XN**2)*(ATP**2)
000175 CALL CS(C1,S1,A1)
000201 F1=CMPLX(.0,4.*XK*XL*(XN**2))+2.*SQRTPI *P(A1)*((2.*XK*XL*(XN**2)
000211 1)*#1.5)*ATP*(P(-PIC4 )-SQRT(2.)*CMPLX(C1,-S1))
CCP=C*F1
11
000273 TM=(PI-BR)/(2.*XN)
000301 ATM=ABS(TM)
000304 IF(ATM.LT. 0.01)GO TO 20
000306 XNM=(BR-PI)/(2.*XN*PI)
000311 NM=XNM
000314 E2=XNM-NM
000316 IF(E2.GT. 0.5)NM=NM+1
000320 IF(E2.LT. -0.5)NM=NM-1
000324 AM=1.+COS(-BR+2.*XN*NM*PI)
000330 XKAM=XK*XL*AM
000344 CM=CEXP(CMPLX(.0,-PI04))/(4.*(XN**2)*SQRT(TWOPI*XK)*(SIN(PI-BR)/
000346

```

000411	1(2.*XN)**2))	71100000
000421	CCM=CM*V(XKAM)	71200000
000425	GO TO 21	71300000
000433	20 A1=2.*XK*XL*(XN**2)*(ATP**2)	71400000
000435	CALL CS(C1,S1,A1)	71500000
	F2=CMPLX(.J,4.*XK*XL*(XN**2))+2.*SQRTPI *P(A1)*((2.*XK*XL*(XN**2)	71600000
	1)*1.5)*ATM*(P(-PI*4 )-SQRT(2.)*CMPLX(C1,-S1))	71700000
000517	CCM=C#F2	71800000
000525	21 IF(T1.EQ. 1 )GO TO 1	71900000
000527	DP=CCP	72000000
000531	DM=-CCM	72100000
000534	IF(T2.EQ. 1 )DP=-CCP	72200000
000540	IF(T2.EQ. 1 )DM=CCM	72300000
000545	GO TO 2	72400000
000546	1 DP=CCP	72500000
000551	DM=-CCM	72600000
000553	2 U=OP+DM	72700000
000550	RETURN	72800000
000561	END	72900000
	COMPLEX FUNCTION V(X)	73000000
C	TRANSITION FUNCTION FOR THE INTEGRAL WITH THE INTEGRAND HAVING THE	73100000
C	POLE OF ORDER TWO CLOSE TO THE SADDLE	73200000
C	X = K*A(BETA)	73300000
	COMPLEX P	73400000
	P(X)=CEXP(CMPLX(.0,X))	73500000
C		73600000
	CCMCMN/PI*CNST/PI, TP,STP,SQRTPI,TT,TTDEG,PI*2,PI*4	73700000
	CALL CS(C,S,X)	73800000
	V=CMPLX(.0,2.*X)+2.*(X**1.5)*P(X)*SQRTPI *(P(-PI*4 )-SQRT(2.))*	73900000
	1CMPLX(C,-S))	74000000
	RETURN	74100000
	END	74200000



0050	RETURN	73000000
0051	2 D=COS(Z)	75000000
0053	S=SIN(Z)	78000000
0061	Z=4./Z	78300000
0063	A=(((((8.768258E-4*Z-4.169289E-3)*Z+7.970943E-3)*Z-6.792801E-3)	79000000
	1*Z-3.095341E-4)*Z+5.972151E-3)*Z-1.606428E-5)*Z-2.493322E-2)*Z	79100000
	2-4.444091E-9	79200000
0100	B=(((((1-6.633926E-4*Z+3.401409E-3)*Z-7.271690E-3)*Z+7.428246E-3)	79300000
	1*Z-4.027145E-4)*Z-9.314910E-3)*Z-1.207998E-6)*Z+1.994711E-1	79400000
0113	Z=SGN(Z)	79500000
000115	C=0.5+Z*(D*A+S*B)	79500000
000125	S=0.5+Z*(S*A-D*B)	79700000
000132	RETURN	79800000
000133	END	

```

SUBROUTINE TFST(N,AL,XS,A,TYPE)
C THIS SUBROUTINE PROGRAM CCMPUTES THE RADIATION FIELD OF HORN ANTENNA
C
000010 DIMENSION X(180),AM(180),AP(180),DC(180),A(180),ANG(180)
000010 DIMENSION THIFD(185),AMPFD(185),DBIFD(185)
000010 CCMPLX F,A,DG,CEG,TAL
000010 COMMON XLAMDA,XPIN,XL,H,RI,RS,THI,DMAX,FIELD,SOURCE
000010 COMMON/PICINST/PI, TP,STP,SQRTPI,TT,TTDEG,PIU2,PIJ4
C XPIN IS POINT OF INCIDENCE WHICH IS X IN MAIN PROGRAM
C
000010 F(Z)=CEXP( CMPLX(0.,-6.2831853071796*Z))/SQRT(6.2831853071796*Z)
000036 FA(SA,SB,SC)= ACOS((SB*SB+SC*SC-SA*SA)/(2.0*SB*SC))
000057 FC(AA,SB,SC)=SQRT((SB*SB+SC*SC-2.0*SB*SC*COS(AA))
000101 FB(SX)=ABS(COS(SX/2.0))*2.0
C
C FB(SX) IS THE OBLIQUITY FACTOR. TO IGNORE IT, SET FB(SX)=1.
C
NN=(N+1)/2
L=0
D=0.0
IF(N.GT.1) D=AL/FLUAT(N-1)
TH=0.0
2 CONTINUE
IF(TH.EQ.90.0) GO TO 15
THR=TH*PI
ANG(1)=THR
X(1)=XS
DG(1)=A(1)*F(XS)*FR(THR)
IF(TYPE.EQ.3.0.AND.THR.LT.PIU2 ) DG(1)=DG(1)*COS(THR)
IF(TYPE.EQ.3.0.AND.THR.GT.PIU2 ) DG(1)=DG(1)*COS(PI-THR)
IF(N.EQ.1) GO TO 11
I=2
3 CONTINUE
X(I)=FC(PI*0.5+THR,FLUAT(I-1)*D,XS)
IF(I.GT.NN) X(I)=FC(PIU2 -THR,FLUAT(I-NN)*D,XS)
IF(TH.GT.90.0) X(I)=FC(1.5*PI-THR,FLUAT(I-1)*D,XS)
IF(TH.GT.90.0.AND.I.GT.NN) X(I)=FC(THR-PIU2 ,FLUAT(I-NN)*D,XS)
ANG(I)=THR+FA(FLUAT(I-1)*D,XS,X(I) )
IF(I.GT.NN) ANG(I)=THR-FA(FLUAT(I-NN)*D,XS,X(I) )
IF(TH.GT.90.0) ANG(I)=THR-FA(FLUAT(I-1)*D,XS,X(I) )
IF(TH.GT.90.0.AND.I.GT.NN) ANG(I)=THR+FA(FLUAT(I-NN)*D,XS,X(I) )

```

```

79900000
80000000
80100000
80200000
80300000
80400000
80500000
80600000
80700000
80800000
80900000
81000000
81100000
81200000
81300000
81400000
81500000
81600000
81700000
81800000
81900000
82000000
82100000
82200000
82300000
82400000
82500000
82600000
82700000
82800000
82900000
83000000
83100000
83200000
83300000
83400000
83500000
83600000
83700000
83800000
83900000
84000000

```



```

000376      DG(I)=A(I)*F(X(I))*FB(ANG(I) )
000377      IF(TYPE.EQ.3.0.AND.ANG(I).LT.PI02 ) DG(I)=DG(I)*COS(ANG(I))
000378      IF(TYPE.EQ.3.0.AND.ANG(I).GT.PI02 ) DG(I)=DG(I)*COS(PI-ANG(I))
000379      IF(I.EQ.N) GO TO 11
000380      I=I+1
000381      GO TO 3
000382
000383      11 CONTINUE
000384      TAL=CMPLX(0.0,0.0)
000385      DO 33 K=1,N
000386      CUS=DG(K)
000387      ANG=ANG(K)*TTDEG
000388      ADG=CABS(CDG)
000389      TAL=TAL+DG(K)
000390
000391      33 CONTINUE
000392      ATAL=CABS(TAL)
000393      IF(TH.EQ.0.0) XNCM=ATAL
000394      DBTAL=20.0*ALOG10(ATAL)
000395      WRITE(6,4) TH,ATAL,CBTAL
000396      4 FORMAT( 5X*TH=*F10.4,5X,*MAGNITUDE= *,E15.4,5X,*DBHA= *,E15.4)
000397      L=L+1
000398
000399      *
000400      THIFD(L)=TH
000401      AMPIFD(L)=ATAL
000402      CBIFD(L)=DBTAL
000403
000404      15 CONTINUE
000405      TH=TH+2.0
000406      IF(TH.LE.360.0) GO TO 2
000407      PRINT 39,(THIFD(J),AMPIFD(J),CBIFD(J), J=1,L)
000408      39 FORMAT(///2X* TH*7X*AMPLITUDE*7X* DBHA*/(F5,2(5XF10.5)))
000409
000410      C FIND MAX AMPIFD
000411      AMAX=AMPIFD(1)
000412      TMAX= THIFD(1)
000413      DO 6596 J=2,L
000414      IF (AMPIFD(J).LE.AMAX) GO TO 6596
000415      AMAX=AMPIFD(J)
000416      TMAX= THIFD(J)
000417
000418      6596 CONTINUE
000419      C NORMALIZE AMPIFD
000420      DO 6597 J=1,L
000421      AMPIFD(J)=AMPIFD(J)/AMAX
000422
000423      6597 CONTINUE
000424      PRINT 5555,AMAX,TMAX
000425      5555 FORMAT(// * MAX AMPIFD=*F9.5, * FOR THIFD=*F3* DEG*)
000426
000427      84100000
000428      84200000
000429      84300000
000430      84400000
000431      84500000
000432      84600000
000433      84700000
000434      84800000
000435      84900000
000436      85000000
000437      85100000
000438      85200000
000439      85300000
000440      85400000
000441      85500000
000442      85600000
000443      85700000
000444      85800000
000445      85900000
000446      86000000
000447      86100000
000448      86200000
000449      86300000
000450      86400000
000451      86500000
000452      86600000
000453      86700000
000454      86800000
000455      86900000
000456      87000000
000457      87100000
000458      87200000
000459      87300000
000460      87400000
000461      87500000
000462      87600000
000463      87700000
000464      87800000
000465      87900000
000466      88000000
000467      88100000
000468      88200000
000469      88300000

```

```

** IN TEST
88400000
88500000
88600000
88700000
88800000
88900000
89000000
89100000
89200000
89300000
89400000
89500000
89600000
89700000
89800000
89900000
90000000
90100000
90200000
90300000
90400000
90500000
90600000
90700000
90800000
90900000
91000000
91100000
91200000

91300000
91400000
91500000
91600000
91700000
91800000
91900000
92000000
92100000
92200000
92300000
92400000
92500000
92600000

10641 FIELD=SHINCID
10642 DMAX=CBIFD(1)
10644 TMAX=THIFD(1)
10646 DO 6598 J=2,L
10652 IF(DBIFD(J)-LE.DMAX) GO TO 6598
10655 DMAX=DBIFD(J)
10656 TMAX=THIFD(J)
10657 6598 CONTINUE
C NORMALIZE DBFA WHICH IS DBIFD
DO 6599 J=1,L
DBIFD(J)=DBIFD(J)-DMAX
IF(CBIFD(J).LT.-40.) CBIFD(J)=-40.
6599 CONTINUE
PRINT 5556,DMAX,TMAX
5556 FORMAT(//'* MAX DBIFD=*F9.5* FOR THIFD=*F3* DEG*')
PRINT 40,(THIFD(J),AMPIFD(J),DBIFD(J),J=1,L)
40 FORMAT(//'* THIFD*5X*AMPIFDNR*7X*CBIFDNR*/(F5,2(4XF10.5)))
CALL POLPLT(THIFD,CBIFD,180,7.5,8,1,N,TYPE,AL,XLAMDA,XPIN,XL,H,RI
1,RS,THI,DMAX,FIELD,SOURCE)
***
THIFD(L+1)=0.
THIFD(L+2)=30.
AMPIFD(L+1)=0.
AMPIFD(L+2)=-1
CALL PLTIFD(THIFD,AMPIFD,180)
RETURN
END

10751 THIFD(L+1)=0.
10753 THIFD(L+2)=30.
10754 AMPIFD(L+1)=0.
10755 AMPIFD(L+2)=-1
10757 CALL PLTIFD(THIFD,AMPIFD,180)
10761 RETURN
10762 END

SUBROUTINE PLTIFD(THSTFD,AMPTFD,NPTS)
DIMENSION THSTFD(1),AMPTFD(1)
TMAJ=1.
TMIN=3.
CALL GJATI(0.00,0.2,-28,11,TOTAL FIELD,0.,11)
CALL CALPLT(0.,1.0,-3)
CALL AXES(0.,0.,50.,10.,0.,0.1,1.,5.,9,HAMPLITUDE,.28,9)
CALL AXES(0.,0.,0.,12.,-180.,30.,TMAJ,TMIN,10,THSTFD,DEJ,-28,-10)
CALL AXES(0.,10.,0.,12.,0.,30.,TMAJ,TMIN,1H,0.,1)
CALL AXES(12.,0.,0.,10.,0.,0.1,1.,5.,1H,0.,-1)
CALL LINE(THSTFD,AMPTFD,NPTS,1,0,0,0.)
CALL VFRAME
RETURN
END

000006
000006
000007
000011
000015
000020
000033
000046
000051
000074
000103
000104
000105

```

```

SUBROUTINE PLTTFDP(THSTFD,PHTFD,NPIS)
DIMENSION THSTFD(1),PHTFD(1)
TMAJ=1.
TMIN=3.
CALL NGTATE(0.00,0.2,.28,11HTOTAL FIELD,0.,11)
CALL CALPLT(0.,1.0,-3)
CALL AXES(0.,0.,90.,12.,-180.,30.,1.,3.,9PHASE,DEG,-28,9)
CALL AXES(0.,0.,0.,12.,-180.,30.,TMAJ,TMIN,10HTSTFD,DEG,-28,-10)
CALL AXES(0.,12.,0.,12.,-180.,30.,TMAJ,TMIN,14,0.,1)
CALL AXES(12.,0.,0.,90.,12.,-180.,30.,1.,3.,14,0.,-1)
CALL LINE(THSTFD,PHTFC,NPIS,1,0,0.)
CALL NFRAME
RETURN
END
92700000
92800000
92900000
93000000
93100000
93200000
93300000
93400000
93500000
93600000
93700000
93800000
93900000
94000000

```

```

SUBROUTINE PULPLT(DEGS,DBS,NPTS,DIAM,NCCIR,NPLOTS,N,TYPE,AL,
1 XLAMDA,X,XL,H,RI,RS,THI,DMAX,FIELD,SOURCE)
*
DIMENSION DEGS(1),DBS(1),CHTAB(16)
DIMENSION ANUM(11),FIELD(2)
DIMENSION COB(400),RHOX(400),RHOY(400),PHI(400)
*
RAD = DIAM/2.0
HGT=.21
*
CHTAB(1) =1H
CHTAB(2) =1H5
CHTAB(3) =2H10
CHTAB(4) =2H15
CHTAB(5) =2H20
CHTAB(6) =2H25
CHTAB(7) =2H30
CHTAB(8) =2H35
*
CALL NOTATE (0.,0.,HGT,3,0.,-1)
RADO =RAD
DELTR=RAD/NOCIR
CX=10.
PX=10.
AY= 5.0
PY=5.
K=1
HGT=.14
*
1 CCNTINUE
DO 5 I=1,NOCIR
RADF=RADO
CALL CIRCLE(CX,AY,0.,360.,RADO,RADF,3)
IF(1.EQ.3)K=2
CALL NOTATE (CX,AY,HGT,CHTAB(1),270.,K)
RADO=RADO-DELTR
CX= CX-DELTR
5 CONTINUE
*** COORDINATES FOR CENTER OF CIRCLE ***
CNTKX=PX-RAD
CNTRY=PY
0026
0026
0026
0026
0027
0031
0032
0034
0035
0037
0040
0042
0043
0045
0051
0052
0060
0061
0062
0063
0064
0065
0067
0067
0071
0073
0101
0110
0116
0120
0121
0127
0130
94100000
94200000
94300000
94400000
94500000
94500000
94700000
94800000
94900000
95000000
95100000
95200000
95300000
95400000
95500000
95600000
95700000
95800000
95900000
96000000
96100000
96200000
96300000
96400000
96500000
96500000
96700000
96800000
96900000
97000000
97100000
97200000
97300000
97400000
97500000
97600000
97700000
97800000
97900000
98000000
98100000
98200000

```

```

000132      ANGLE=-.174532925
000133      TIC=.1
000135      RPT=RAC+TIC
000136      DELTA=-.174532525

***      *
***      *      DRAW TIC MARKS EVERY 10 DEGREES      ***
*

000140      DO 50 I=1,36
***      *
***      *      PAGE COORDINATES      ***
*      TICX1=CNTRX+RAD* COS (ANGLE)
*      TICY1=CNTRY+RAD* SIN (ANGLE)
*      TICX2=CNTRX+RPT* COS (ANGLE)
*      TICY2=CNTRY+RPT* SIN (ANGLE)
*      CALL CALPLT (TICX1,TICY1,3)
*      CALL CALPLT (TICX2,TICY2,2)
*      ANGLE=ANGLE+DELTA
*      50 CONTINUE
***      *
***      *      DRAW LABLES      ***
*

000202      ANUM(1)=N
000203      ANUM(2)=TYPE
000205      ANUM(3)=AL
000206      ANUM(4)=XLAMDA
000210      ANUM(5)=X
000211      ANUM(6)=XL
000213      ANUM(7)=H
000214      ANUM(8)=RI
000216      ANUM(9)=RS
000217      ANUM(10)=THI/ (.1*DELTA)
000222      ANUM(11)=D*MAX
000224      CALL NOTATE (11.40,9.0,-.21,14)HTTRANSMITTED WL=,270.,14)
000230      CALL NUMBER (11.40,6.5,.21,ANUM(4),270.,-1)
000236      CALL NOTATE (11.40,4.3,.21,12)HNCID RANGE=,270.,12)
000242      CALL NUMBER (11.40,2.0,.21,ANUM(8),270.,2)
000250      CALL NOTATE (11.10,5.0,.21,12)HNCID POINT=,270.,12)
000254      CALL NUMBER (11.10,6.7,.21,ANUM(5),270.,2)
000262      CALL NOTATE (11.10,4.3,.21,12)HSCATER RNGE=,270.,12)
000266      CALL NUMBER (11.10,2.0,-.21,ANUM(9),270.,-1)
000274      CALL NOTATE (10.80,5.0,.21,11)HBOX LENGTH=,270.,11)
000300      CALL NUMBER (10.80,6.9,.21,ANUM(6),270.,2)
000306      CALL NOTATE (10.80,4.3,.21,12)HNCID ANGLE=,270.,12)
000312      CALL NUMBER (10.80,2.0,.21,ANUM(10),270.,-1)
98300000
98400000
98500000
98600000
98700000
98800000
98900000
99000000
99100000
99200000
99300000
99400000
99500000
99600000
99700000
99800000
99900000
10000000
10010000
10020000
10030000
10040000
10050000
10060000
10070000
10080000
10090000
10100000
10110000
10120000
10130000
10140000
10150000
10160000
10170000
10180000
10190000
10200000
10210000
10220000
10230000
10240000
10250000

```

000320	CALL NOTATE(10.50,9.0,.21,11HBOX HEIGHT=,270.,11)	102500000
000324	CALL NUMBR(10.50,6.9,.21,ANUM(7),270.,-1)	102700000
000332	CALL NOTATE(10.50,4.3,.21,12HNORMALIZ D3=,270.,12)	102800000
000336	CALL NUMBR(10.50,2.0,.21,ANUM(11),270.,3)	102900000
000344	CALL NOTATE(1.70,4.3,.21,15HLINE SOURCES,N=,270.,15)	103000000
000350	CALL NUMBR(1.70,1.6,.21,ANUM(1),270.,-1)	103100000
000356	CALL NOTATE(1.40,4.8,.21,20H CURNT TYPE=,270.,20)	103200000
000362	CALL NUMBR(1.40,1.2,.21,ANUM(2),270.,-1)	103300000
000370	CALL NOTATE(1.40,4.8,.21,SOURCE,270.,9)	103400000
000375	CALL NOTATE(1.10,9.0,.21,11H FIELD,270.,11)	103500000
000401	CALL NOTATE(1.10,9.0,.21,FIELD,270.,5)	103600000
000406	CALL NOTATE(1.10,4.0,.21,12HAPERT WIDTH=,270.,12)	103700000
000412	CALL NUMBR(1.10,1.75,.21,ANUM(3),270.,3)	103800000
	*** DRAW X AXIS	103900000
000420	AX=PX-DIAM-.5	104000000
000427	CALL CALPLT(AX,AY,3)	104100000
000431	AX=PX+.5	104200000
000433	CALL CALPLT(AX,AY,2)	104300000
	*** DRAW ZERO DEGREES AFTER HORIZONTAL	104400000
000436	HGT=.21	104500000
000437	AX=PX	104500000
000441	AY=AY-.05	104700000
000443	CALL NOTATE (AX,AY,HGT,1H0,270.,1)	104800000
000447	AX=AX+.21	104900000
000451	AY=AY-.12	105000000
	*** DEGREE SYMBOL	105100000
000453	CALL NOTATE (AX,AY,.07,1H0,270.,1)	105200000
	***DRAW Y AXIS	105300000
000457	AY=5.0	105400000
000460	AX= PX-RAD	105500000
000462	AY= AY-RAD-.5	105600000
000466	CALL CALPLT(AX,AY,3)	105700000
000470	AY=AY+ DIAM+1.	105800000
000476	CALL CALPLT(AX,AY,2)	105900000
	***DRAW 90 DEGS	106000000
000501	AY=AY-.1	106100000
000503	CALL NOTATE(AX,AY,HGT,2H90,270.,2)	106200000
000507	AX=AX+HGT	106300000
000511	AY=AY-.32	106400000
000513	CALL NOTATE (AX,AY,.07,1H0,270.,1)	106500000
	*** DRAW 180 DEGREES	106600000
000517	AX=PX-DIAM-.3	106700000
000525	AY=5.0	106800000

000527	CALL NCTATE (AX,AY,PGT,3H180,270.,3)	106900000
000533	AX=AX+.21	107000000
000535	AY=AY-.5	107100000
000537	CALL NCTATE (AX,AY,.07,1H0,270.,1)	107200000
*		107300000
***DRAW 270 DEGS		107400000
000543	AX=PX-RAD	107500000
000545	AY=5.0-RAD-.05	107600000
000550	CALL NCTATE(AX,AY,HGT,3H270,270.,3)	107700000
000554	AX=AX+HGT	107800000
000556	AY=AY-.5	107900000
000560	CALL NCTATE (AX,AY,.07,1H0,270.,1)	108000000
*		108100000
**		108200000
*		108300000
000554	151 CONTINUE	108400000
*		108500000
***PLOT POLAR CURVES ***		108600000
*		108700000
***SCALE DECIBELS AND CONVERT POLAR COORDINATES TO CART. COORDS.		108800000
000564	DC 500 JJ=1,NPTS	108900000
000571	PHI=DEGS(JJ)*.0174532925	109000000
000573	CCB(JJ)=DAS(JJ)+40.	109100000
000576	CCB(JJ)=.025*RAU*CCB(JJ)	109200000
000581	RHOX(JJ)=CCB(JJ)*COS(PHI)	109300000
000610	RHOY(JJ)=CCB(JJ)*SIN(PHI)	109400000
000616	500 CONTINUE	109500000
000624	LI M=NPTS-1	109600000
***BEGIN PLOTTING WITH PEN UP***		109700000
000625	IPEN=3	109800000
000627	DO 100 I=1,LIM	109900000
000630	J=I+1	110000000
000632	CALL CIRCLE(RHOX(I),RHOY(I),DEGS(I),DEGS(J),CCB(I),CCB(J),IPEN)	110100000
000655	IF(I.GT.1)GO TO 110	110200000
000664	IPEN=2	110300000
000655	110 CONTINUE	110400000
000665	100 CONTINUE	110500000
*		110600000
000670	CALL NFRAME	110700000
000671	RETURN	110800000
000672	END	110900000

```

111000000
111100000
111200000
111300000
111400000
111500000
111600000
111700000
111800000
111900000
112000000
112100000
112200000
112300000

```

```

SUBROUTINE PLTIFD(THIFD,AMPIFD,NPTS)
DIMENSION THIFD(1),AMPIFD(1)
TMAJ=1.
TMIN=3.
CALL ROTATE(0.00,0.2,-.28,14HINCIDENT FIELD,0.,14)
CALL CALPT(0.,1.0,-3)
CALL AXES(0.,0.,90.,10.,0.,0.1,1.,5.,9AMPLITUDE,.28,9)
CALL AXES(0.,0.,0.,12.,0.,30.,TMAJ,TMIN,9THIFD,DEG,.28,-9)
CALL AXES(0.,1),0.,12.,-180.,30.,TMAJ,TMIN,1H,0.,1)
CALL AXES(12.,0.,90.,10.,0.,0.1,1.,5.,1H,0.,-1)
CALL LINE(THIFD,AMPIFD,180,1,0,0,0.)
CALL NFRAME
RETURN
END

```

```

000006
000006
000007
000011
000019
000023
000033
000046
000061
000074
000104
000105
000106

```



## REFERENCES

1. Keller, J. B., "Geometrical Theory of Diffraction," J. Opt. Soc. Am., 52, pp. 116-130, 1962.
2. Meil, K. K. and Van Bladel, J. G., "Scattering by Perfectly-Conducting Rectangular Cylinders," IEEE Trans, AP-11, pp. 185-192, 1963.
3. Andreasen, M. G. and Mei, K. K., "Scattering by Conducting Cylinders," IEEE Trans, AP-12, pp. 235-236, 1964.
4. Morse, B. J., "Diffraction by Polygonal Cylinders," J. Math. Phys., 5, pp. 199-214, 1964.
5. Oberhettinger, F., "On Asymptotic Series for Functions Occurring in the Theory of Diffraction of Waves by Wedges," J. Math. Phys., 34, pp. 245-255, 1956.
6. Pathak, P. H. and Kouyoumjian, R. G., "The Dyadic Diffraction Coefficient for a Perfectly-Conducting Wedge." Report 2183-4, June 1970, The Ohio State University ElectroScience Laboratory, Department of Electrical Engineering; prepared under Contract AF 19(628)-5929 for Air Force Cambridge Research Laboratories. (AFCRL-69-0546) (AD 707 827)
7. Kouyoumjian, R. G. and Pathak, P. H., "The Dyadic Diffraction Coefficient for a Curved Edge." NASA CR-2401, 1974.
8. Karp. S. N. and Keller, J. B., "Multiple Diffraction by an Aperture in a Hard Screen," Optica Acta, 8, pp. 61-72, 1961.



POSTMASTER : If Undeliverable (Section 158  
Postal Manual) Do Not Return

*"The aeronautical and space activities of the United States shall be conducted so as to contribute . . . to the expansion of human knowledge of phenomena in the atmosphere and space. The Administration shall provide for the widest practicable and appropriate dissemination of information concerning its activities and the results thereof."*

—NATIONAL AERONAUTICS AND SPACE ACT OF 1958

## NASA SCIENTIFIC AND TECHNICAL PUBLICATIONS

**TECHNICAL REPORTS:** Scientific and technical information considered important, complete, and a lasting contribution to existing knowledge.

**TECHNICAL NOTES:** Information less broad in scope but nevertheless of importance as a contribution to existing knowledge.

**TECHNICAL MEMORANDUMS:** Information receiving limited distribution because of preliminary data, security classification, or other reasons. Also includes conference proceedings with either limited or unlimited distribution.

**CONTRACTOR REPORTS:** Scientific and technical information generated under a NASA contract or grant and considered an important contribution to existing knowledge.

**TECHNICAL TRANSLATIONS:** Information published in a foreign language considered to merit NASA distribution in English.

**SPECIAL PUBLICATIONS:** Information derived from or of value to NASA activities. Publications include final reports of major projects, monographs, data compilations, handbooks, sourcebooks, and special bibliographies.

**TECHNOLOGY UTILIZATION PUBLICATIONS:** Information on technology used by NASA that may be of particular interest in commercial and other non-aerospace applications. Publications include Tech Briefs, Technology Utilization Reports and Technology Surveys.

*Details on the availability of these publications may be obtained from:*

**SCIENTIFIC AND TECHNICAL INFORMATION OFFICE  
NATIONAL AERONAUTICS AND SPACE ADMINISTRATION  
Washington, D.C. 20546**